Biochimica et Biophysica Acta, 934 (1988) 348–368
Elsevier

BBA 42801

Light-induced proton uptake by photosynthetic reaction centers from *Rhodobacter sphaeroides* R-26. I. Protonation of the one-electron states $D^+Q_A^-$, DQ_A^-, $D^+Q_AQ_B^-$, and $DQ_AQ_B^-$ *

P.H. McPherson, M.Y. Okamura and G. Feher

Department of Physics, University of California, San Diego, La Jolla, CA (U.S.A.)

(Received 11 January 1988)

Key words: Bacterial photosynthesis; Reaction center; Proton uptake; Redox midpoint potential; Chemiosmotic hypothesis; (*Rb. sphaeroides*)

The proton uptake associated with the light-induced transfer of an electron to the acceptor quinones Q_A and Q_B was investigated in reaction centers from *Rhodobacter sphaeroides* R-26. The proton uptake was found to be pH dependent with maximum values of approx. 0.5 H^+/e^- at pH 9 for DQ_A^- and approx. 0.8 H^+/e^- at pH 10 for $DQ_AQ_B^-$. The quinones are not protonated directly. The observed proton uptake is due to shifts in the pK values of amino acid residues that interact with the quinones. The pH-dependences of the proton uptake were fitted with a phenomenological model in which the protons are taken up by four amino acid residues. The deduced pK shifts associated with the reductions of the quinones ranged from 0.4 to 0.8 for Q_A and from 0.4 to 1.3 for Q_B. The proton uptake by $D^+Q_A^-$ and $D^+Q_AQ_B^-$ was less than that by DQ_A^- and $DQ_AQ_B^-$, respectively, indicating a release of protons associated with the formation of D^+. To calculate the pH-dependence of the redox midpoint potentials of Q_A ($E_{m(Q_A)}$) and Q_B ($E_{m(Q_B)}$) from the proton uptake, we used a thermodynamic (model-independent) relation. $E_{m(Q_A)}$ decreased approx. 20 mV/pH at 6.0 < pH < 10.5, while $E_{m(Q_B)}$ decreased approx. 20 mV/pH at 6.0 < pH < 8.5 and approx. 40 mV/pH at pH < 6.0 and pH > 9.0. The pH dependence of $E_{m(Q_A)}$ in isolated reaction centers is significantly weaker than that determined from redox titrations of Q_A in chromatophores of *Rb. sphaeroides* (see for example Prince, R.C. and Dutton, P.L. (1976) Arch. Biochem. Biophys. 172, 329–334). The pH-dependence of the free energy between $Q_A^-Q_B$ and $Q_AQ_B^-$ obtained from the difference of $E_{m(Q_A)}$ and $E_{m(Q_B)}$ is in good agreement with that determined from the measurement of electron-transfer kinetics in isolated RCs from *Rb. sphaeroides* (Kleinfeld, D., Okamura, M.Y., and Feher, G. (1984) Biochim. Biophys. Acta 766, 126–140). The stronger average interaction of the protons with Q_B^- provides the driving force for the forward electron transfer. A simplified model was used to calculate the pK shifts from the electrostatic energy between Q_A^- or Q_B^- and the charges of the protonatable amino acid residues whose positions were obtained from the three-dimensional structure (Allen, J.P., Feher, G., Yeates, T.O., Komiya, H. and Rees, D.C. (1987) Proc. Natl. Acad. Sci. USA 84, 6162–6166).

* This work was performed in partial fulfillment for the Ph.D. degree of P.H. McPherson.

Abbreviations: D, primary donor; Q_A, primary acceptor; Q_B, secondary acceptor; RC, reaction center; UQ-10, ubiquinone-50; BChl, bacteriochlorophyll; LDAO, lauryldimethylamine *N*-oxide; Pipes, 1,4-piperazinediethanesulfonic acid; Tris, 2-amino-2-hydroxymethylpropane-1,3-diol; Ches, cyclohexylaminoethanesulfonic acid.

Correspondence: G. Feher, Department of Physics, University of California, San Diego, B-019, La Jolla, CA 92093, U.S.A.

Introduction

The primary process of photosynthesis, i.e., the conversion of light into electrochemical energy, is mediated by an integral membrane protein-pigment complex called the reaction center (RC). Reaction centers isolated from the bacterium *Rhodobacter sphaeroides* R-26 consist of three protein subunits (L, M and H) and several cofactors: four bacteriochlorophylls, two bacteriopheophytins, one non-heme iron (Fe^{2+}) and two ubiquinones (UQ-10) (for reviews, see Refs. 1–3). The amino acid sequence [4–6] and three-dimensional structure [7,8] of this RC have been determined.

The absorption of a photon by the RC produces a charge separation that is temporally stabilized by the serial transfer of the electron through an acceptor complex *:

$$DQ_AQ_B \xrightarrow{h\nu} D^+Q_A^-Q_B \rightarrow D^+Q_AQ_B^- \quad (1)$$

where D is the primary donor (BChl dimer) and Q_A and Q_B are the primary and secondary acceptors (UQ-10 molecules), respectively (for reviews, see Refs. 9 and 10). The subsequent reduction of D^+ by a secondary, exogenous, donor (cytochrome c_2^{2+}) produces the species $DQ_AQ_B^-$, which can absorb a second photon, thereby generating $DQ_AQ_B^{2-}$. In vivo, the two electrons are transferred out of the reaction center to a ubiquinone pool (see, e.g., Ref. 11). This process provides the driving force for proton transport across the membrane, forming a chemiosmotic gradient that drives ATP synthesis (for reviews, see Refs. 12 and 13).

In this work we are concerned with the proton uptake that accompanies the transfer of the first electron to Q_A and Q_B (i.e., Eqn. 1). In a forthcoming paper (No. II in this series), we will examine the proton uptake associated with the two-electron state $DQ_AQ_B^{2-}$.

The importance of the protonation of the one-electron states is two-fold: (i) it is related to the free-energy difference between $Q_A^-Q_B$ and $Q_AQ_B^-$ [14,15] and therefore affects the direction and kinetics of electron transfer; (ii) it may play a role in the formation of the chemiosmotic potential.

The proton uptake associated with the one-electron states in RCs from *Rb. sphaeroides* has been investigated by several authors using a variety of approaches, but so far no consensus on the stoichiometry has been reached. These approaches include: (i) Direct measurement in isolated RCs [14,16–20]. The reported values for the proton uptake at pH 7.5 by DQ_A^- range from 0.3 to 0.6 protons per electron (H^+/e^-) and by $DQ_AQ_B^-$ from approx. 0 to 0.8 H^+/e^-. (ii) Determination of the pH dependence of the redox midpoint potentials of Q_A and Q_B by redox titration [21–25]. The proton uptake was deduced from the pH-dependence of the midpoint potential of Q_A in chromatophores [21–23] or RCs incorporated into liposomes [24]. The deduced value of proton uptake of 1 H^+/e^- at pH $\lesssim$ 10 is a factor of approx. 2–3 larger than measured in isolated RCs. The pH dependence of the midpoint potential of Q_B has not been determined in sufficient detail to reach a conclusion about the protonation of Q_B [25]. (iii) Determination of the pH dependence of the free energy between the states $Q_A^-Q_B$ and $Q_AQ_B^-$ from the electron-transfer kinetics in isolated RCs [15]. The proton uptake was deduced from a model fitted to the kinetics data. An uptake of 1 H^+/e^- at pH $\lesssim$ 10 was deduced for the reduction of Q_A, consistent with the redox titrations. An uptake of 1 H^+/e^- at pH $\lesssim$ 11 was deduced for the reduction of Q_B as well.

In view of the disagreement between the results obtained by the different methods, we reexamined the proton uptake by a direct measurement of the pH changes (with a glass electrode) accompanying the formation of the one-electron states: $D^+Q_A^-$, DQ_A^-, $D^+Q_AQ_B^-$ and $DQ_AQ_B^-$. We obtained the pH dependence of the proton uptake by all four states and deduced the separate contributions of D^+, Q_A^- and Q_B^-. Using a thermodynamic, i.e., model-independent, relation we determined from the proton uptakes the pH dependences of the free-energy changes that accompany the reduction of the quinones. The pH dependence of the energy difference between $Q_A^-Q_B$ and $Q_AQ_B^-$ is in good agreement with that obtained by Kleinfeld et al.

* An intermediate state, $D^+I^-Q_AQ_B$, where I is Bacteriopheophytin, has been omitted for simplicity in Eqn. 1.

[15]. The results of the proton uptake are in fair agreement with those obtained with isolated RCs by other workers [14,16,18–20]. The discrepancy between the values of proton uptake determined by us and Kleinfeld et al. [15] is attributed to an improperly chosen model in Ref. 15.

The large difference between the pH dependence of the midpoint potential of Q_A in isolated RCs and chromatophores and liposomes remains. Although a possible explanation for this difference has been advanced, this point warrants further investigation.

The optical absorption [26–28] and EPR [29] spectra in RCs from *Rb. sphaeroides* are indicative of the semiquinone anion; i.e., protons do not bind directly to either Q_A^- or Q_B^-. The observed proton uptake is believed to be due to a shift in the pK values of protonatable amino acid residues that interact with Q_A^- and Q_B^- [14]. We developed a phenomenological model to fit the observed pH dependence of the proton uptake. We have also attempted to identify the residues involved in proton uptake by calculating the electrostatic interactions (and associated pK shifts) between Q_A^- or Q_B^- and the charges of the protonatable amino acid residues whose positions were obtained from the three-dimensional structure [7,8]. We used a simplified model neglecting interactions between charged residues and screening by counterions. Consequently, the calculated values were overestimated.

A preliminary account of this work has been presented [30].

Materials and Methods

Reagents and buffers. Solutions of potassium ferricyanide ($K_3Fe(CN)_6$) and potassium ferrocyanide ($K_4Fe(CN)_6$) (Fisher) were prepared in double-distilled water prior to use. Solutions of hydrochloric acid (HCl) were prepared from a 0.01000 ± 0.00005 M stock solution (Fisher). Cytochrome c (Cyt c; horse heart grade VI, Sigma) was reduced (more than 98%) by hydrogen gas in the presence of platinum black (Aldrich) and purified by filtration (cellulose acetate; Milli-pore). The concentration of cytochrome c^{2+} (in 5 mM dipotassium phosphate/45 mM potassium chloride, pH 7.0) was determined from the extinction coefficient $\varepsilon^{550}_{\text{Cyt } c^{2+}} - \varepsilon^{550}_{\text{Cyt } c^{3+}} = 18.5 \text{ mM}^{-1} \cdot \text{cm}^{-1}$ [31] and the change in absorption at 550 nm by oxidation with $K_3Fe(CN)_6$. The following pH buffers were used: 1,4-piperazinediethanesulfonic acid (Pipes; Calbiochem-Behring), $6.0 < \text{pH} < 7.5$; 2-amino-2-hydroxymethylpropane-1,3-diol (Tris-HCl; Schwarz/ Mann), $7.5 < \text{pH} < 8.5$; and cyclohexylaminoethanesulfonic acid (Ches; Calbiochem-Behring), $8.5 < \text{pH} < 10.5$.

Reaction centers. Reaction centers were isolated from *Rb. sphaeroides* R-26 as described [1]. The concentration of RCs was determined from the absorption at 802 nm and the extinction coefficient $\varepsilon^{802} = 288 \text{ mM}^{-1} \cdot \text{cm}^{-1}$ [32]. The reaction centers contained 1.92 ± 0.06 quinones as determined by averaging the results of a Cyt c photooxidation and a donor recovery ($D^+ \rightarrow D$) assay (see, e.g., Ref. 33). The fraction ($\delta = 0.08$) with less than 2 quinones had lost Q_B during isolation. For some experiments, reaction centers (designated 'Q_B-depleted') were prepared without Q_B as described [34]. Different preparations contained 0.59 ± 0.01, 0.78 ± 0.02 or 0.96 ± 0.02 quinones. RCs were typically solubilized in the detergent lauryldimethylamine *N*-oxide (LDAO, Onyx), but in some experiments dodecyl-β-D-maltoside (Calbiochem-Behring) was substituted by extensive dialysis against a solution containing 0.040% dodecyl-β-D-maltoside, 10 mM Tris-HCl and 0.1 mM EDTA at pH 8.0.

Optical measurements. Absorption spectra were recorded on a Cary 17D spectrophotometer (Varian). The kinetics of absorption changes were determined using a single-beam spectrophotometer of local design [15,35]. Optical measurements were made in 10 mM Tris-HCl and 0.025% (w/v) LDAO at pH 8.0 and $23 \pm 1°$C, unless otherwise indicated.

Light source. Continuous illumination was provided by a projector (Leitz; 500 watt tungsten bulb) whose beam passed through water (3 cm), a color filter (Corning c 2-64; transmission at least 50% at $\lambda > 650$ nm), and an interference filter (Corion BB850; band width, 50 nm). The intensity of the light was varied by adding neutral density filters (optical density, 0.3–2.0; Oriel) and was measured with a radiometer (YSI industries). Light-flashes were provided by a pulsed-dye laser (Phase R DL 2100; 0.4 μs flash width, 0.2 J per flash, $\lambda_0 = 590$ nm).

Measurement of proton uptake. Proton uptake was determined from changes in pH by measuring the potential across a glass/calomel combination electrode (Corning No. 476223) with an operational amplifier (Burr-Brown 3528; input impedance: 10^{14} Ω). Data were filtered with a time constant of 100 ms, amplified by a factor of 10, and recorded on a digital oscilloscope (Nicolet Instr. Corp. model 201). The concentration of the reference electrolyte in the calomel electrode was reduced to 50 mM KCl to improve the signal-to-noise ratio. The sensitivity and response time of the apparatus were $3 \cdot 10^{-4}$ pH units and 2 s, respectively.

The low concentration of the reference electrolyte made the calomel electrode sensitive to the difference between the ionic compositions of the pH buffers and the RC solution (see, e.g., Ref. 36). Absolute values of pH were, therefore, determined by calibrating the electrode against a second combination electrode (Radiometer GK2401B; reference electrolyte: 3 M KCl), which was calibrated with pH buffers (Fisher) at integral values in the range 5–11 *.

The changes in potential were calibrated in terms of proton uptake by injecting known amounts of HCl with a Hamilton syringe (model 8001; 10 µl capacity). In order to ensure that the change in potential was proportional to the number of added protons, at least four injections of the same volume (either 5 or 10 µl) but with different normalities of HCl ($[1.00–8.00 \pm 1\%] \cdot 10^{-4}$ M) were performed.

The solution of reaction centers or cytochrome *c* (2 ml) was contained in a cylindrical quartz cell (diameter, 1 cm) and stirred with a magnetic bar. Absorption of carbon dioxide was prevented by a flow of wet nitrogen gas over the surface. The cell and electrode were shielded from stray light and electrical interference by a grounded metal box with a hole to pass the incident light.

Theoretical models and data analysis

Model for the pH-dependence of proton uptake

As discussed in the introduction, spectroscopic evidence indicates that the quinones are not protonated directly [26–29]. Furthermore, the uptake of a fractional proton as well as the shape of the proton uptake curves as a function of pH led to the suggestion that the proton is associated with nearby amino acid residues whose pK values are affected by the redox state of the quinone [14].

We start with a discussion of a single residue in the vicinity of the quinone that can be protonated. The results can easily be extended to a set of non interacting residues whose contributions are computed independently. The reactions are modeled by the basic four-state equilibrium scheme:

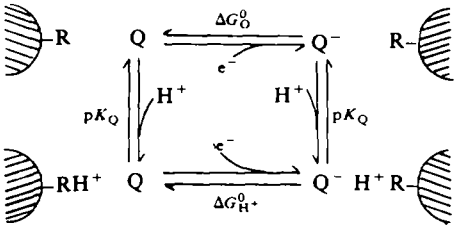

(2)

where H^+ is schematically shown to be associated with a residue R of the reaction center protein (shown cross-hatched); ΔG^0 with their respective subscripts are the standard free energies between the states and pK_Q and pK_{Q^-} are the acid dissociation constants of the residue interacting with Q and Q^-, respectively.

The proton uptake of the system described by Eqn. 2 is shown in Fig. 1. Panel (a) shows the pH dependence of the mole fraction of bound protons for the two states Q and Q^- for an arbitrarily chosen difference $pK_{Q^-} - pK_Q = 1$. The mole fraction is given by the relations:

$$[H^+]_Q = \frac{1}{1+10^{pH-pK_Q}} \tag{3a}$$

$$[H^+]_{Q^-} = \frac{1}{1+10^{pH-pK_{Q^-}}} \tag{3b}$$

The net proton uptake, $\Delta H^+_{Q \to Q^-}$, is given by the difference between Eqn. 3b and Eqn. 3a and is shown in Fig. 1b. It exhibits a peak at the pH equal to the average of pK_Q and pK_{Q^-}. The value of the proton uptake at the peak depends on the difference between pK_Q and pK_{Q^-}. Only for large difference in pK will one proton per electron be taken up. This situation is expected to prevail if

* The electrode showed a difference of approx. 0.2 pH units between the RC solution and pH buffer that was at the same pH (as determined with the second combination electrode).

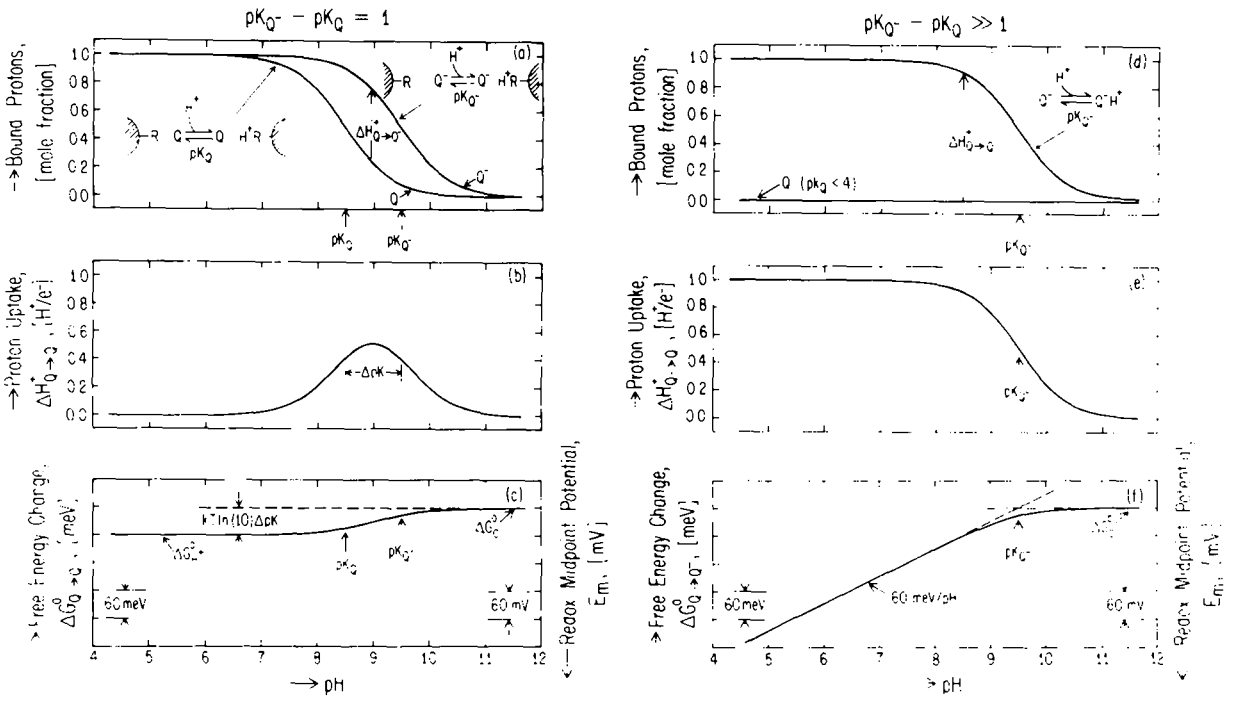

Fig. 1. Proton uptake and free-energy change associated with the electron-transfer reaction $Q \rightarrow Q^-$ for a single protonatable group. Two cases, $pK_{Q^-} - pK_Q = 1$ (left panels) and $pK_{Q^-} - pK_Q \gg 1$ (right panels), are shown. (a) Mole fraction of bound protons for the two states Q and Q^-. The difference between pK_Q and pK_{Q^-} is expected to be small if Q is not protonated directly but instead the proton associates with a residue (R) of the reaction-center protein (shown cross-hatched). (b) Proton uptake given by the difference between the two curves in (a); its value at the peak (at pH = $(pK_Q + pK_{Q^-})/2$) is determined by the difference $\Delta pK = pK_{Q^-} - pK_Q$. (c) Free-energy change $\Delta G^0_{Q \rightarrow Q^-}$. The difference between the asymptotic values ΔG^0_O and $\Delta G^0_{H^+}$ is the stabilization energy of Q^- by the proton. (d–f) Same as (a–c), except that $pK_Q \ll 4$ and $\Delta pK \gg 1$, as expected if the proton were to bind directly to the quinone. In this case, the free-energy change in the region $pK_Q \ll pH \ll pK_{Q^-}$ exhibits a slope of 60 meV/pH at $T = 300$ K, corresponding to an uptake of one proton per electron. In isolated RCs the situation shown in (a–c) prevails.

the quinone were protonated directly, and is depicted in Fig. 1d and 1e.

The above analysis can be generalized to several protonatable non-interacting residues, each being associated with different acid dissociation constants pK_{iQ} and pK_{iQ^-}. The observed proton uptake is given by the sum of the individual contributions:

$$\Delta H^+_{Q \rightarrow Q^-} = \sum_{i=1}^{i=n} \left(\frac{1}{1 + 10^{pH - pK_{iQ^-}}} - \frac{1}{1 + 10^{pH - pK_{iQ}}} \right) \qquad (4)$$

pH-dependence of the free energy change associated with the electron transfer reaction $Q \rightarrow Q^-$

We start again by considering the case of one protonatable residue as shown in Eqn. 2. The free-energy change includes contributions from both the protonated and unprotonated states of Q and Q^- and is given by the Nernst equation:

$$\Delta G^0_{Q \rightarrow Q^-} = -kT \ln \frac{[Q^-]_{H^+} + [Q^-]}{[Q]_{H^+} + [Q]} \qquad (5)$$

where $[Q]_{H^+}$ and $[Q^-]_{H^+}$ are the concentrations of the protonated and [Q] and $[Q^-]$ the unprotonated species. When the concentrations of the four species are written in terms of their respective pK values, Eqn. 5 becomes:

$$\Delta G_{Q \rightarrow Q^-} = \Delta G^0_O - kT \ln \frac{1 + 10^{pK_{Q^-} - pH}}{1 + 10^{pK_Q - pH}} \qquad (6)$$

where ΔG^0_O is given by the expression $-kT \ln([Q^-]/[Q])$ and is independent of pH. Eqn. 6 describes an S-shaped curve with turning points

at pH values equal to pK_Q and pK_{Q^-} (see Fig. 1c). The asymptotic values of Eqn. 6 for high and low pH are given by:

$$pH \gg pK_Q, pK_{Q^-}; \quad \Delta G^0_{Q\to Q^-} = \Delta G^0_O \tag{7}$$

$$pH \ll pK_Q, pK_{Q^-}; \quad \Delta G^0_{Q\to Q^-} = \Delta G^0_{H^+} = \Delta G^0_O - kT\,(\ln 10)\,(pK_{Q^-} - pK_Q) \tag{8}$$

The difference between Eqns. 7 and 8 (i.e., $\Delta G^0_O - \Delta G^0_{H^+}$) represents the stabilization energy of Q^- by the proton.

A special situation that is often encountered arises when $pK_Q \ll pK_Q$. In this case, Eqn. 6 takes on the limiting form in the region $pK_Q \ll pH \ll pK_{Q^-}$:

$$\Delta G^0_{Q\to Q^-} = \Delta G^0_O - kT\,(\ln 10)\,(pK_{Q^-} - pH) \tag{9}$$

Eqn. 9 describes a line with a slope of 60 meV/pH (for $T = 300$ K) that intersects the horizontal line of ΔG^0_O at $pH = pK_{Q^-}$ (Fig. 1f). The line also intersects the horizontal line of $\Delta G^0_{H^+}$ at $pH = pK_Q$. However, since $pK_Q \ll 4$, this is not shown in Fig. 1f. The 60 meV/pH corresponds to an uptake of one proton per electron.

The above analysis can be extended to several protonatable non-interacting residues by summing the individual contributions from each residue as was done for the proton uptake model (Eqn. 4). However, for this case it is advantageous to use an alternate relation between proton uptake and the free-energy change given by (see Appendix A):

$$\Delta G^0_{Q\to Q^-} = kT(\ln 10)\int_{pH}[\Delta H^+_{Q\to Q^-}]\,d(pH) + \Delta G^0 \tag{10}$$

where ΔG^0 is the integration constant corresponding to the energy at which the integration is started. The advantage of Eqn. 10 is that it is model-independent, i.e., it does not depend on the number of protonatable residues, their acid dissociation constants or whether they interact or not.

Analysis of the proton uptake data

The electron-transfer reactions that we investigated are shown in Table I (numbered 1–6). Under each reaction is the expression for the observed proton uptake, ΔH^+_{obs}, from which the proton uptake for a particular state (shown in bold face) was derived.

In several reactions cytochrome c^{2+} was used as an electron donor to D^+. When cytochrome c^{2+} is oxidized protons are released that have to be taken into account. Reaction 1 (Table I) was used to quantitate this proton release.

The proton uptake by $D^+Q_A^-$ in RCs from which the secondary acceptor Q_B had been removed was observed directly (reaction 2, Table I). The proton uptake by DQ_A^- was determined by adding cytochrome c^{2+} to reduce D^+ (reaction 3, Table I). It is given by:

$$\Delta H^+_{DQ_A^-} = \Delta H^+_{obs} - \Delta H^+_{Cyt\,c^{3+}} \tag{11}$$

where $\Delta H^+_{Cyt\,c^{3+}}$ is the cytochrome contribution that was determined independently in reaction 1 (Table I). An alternative method of determining the proton uptake $\Delta H^+_{DQ_A^-}$ in which the cytochrome remains reduced due to the presence of ferrocyanide is shown in reaction 4 (Table I).

The proton uptake by $D^+Q_AQ_B^-$ was obtained from the observed proton uptake of reaction 5 (Table I) and the relation:

$$\Delta H^+_{D^+Q_AQ_B^-} = \frac{\Delta H^+_{obs} - (\alpha - \alpha\delta + \delta)\Delta H^+_{D^+Q_A^-}}{(1-\alpha)(1-\delta)} \tag{12}$$

where δ is the fraction of reaction centers that lack Q_B (see the Materials and Methods section) and α is the pH-dependent partition coefficient between the species $Q_A^-Q_B$ and $Q_AQ_B^-$, i.e., $\alpha = [Q_A^-Q_B]/([Q_A^-Q_B] + [Q_AQ_B^-])$. The value of α had been determined in an independent set of experiments by Kleinfeld et al. [15]. Eqn. 12 was obtained by re-arranging the expression for ΔH^+_{obs} in Table I (reaction 5) and assuming that the proton uptake by $D^+Q_A^-Q_B$ is the same as that by $D^+Q_A^-$. The proton uptake by $DQ_AQ_B^-$ (reaction 6, Table I) observed in the presence of cytochrome c^{2+} was obtained from an expression similar to Eqn. 12:

$$\Delta H^+_{DQ_AQ_B^-} = \frac{\Delta H^+_{obs} - (\alpha - \alpha\delta + \delta)\Delta H^+_{DQ_A^-} - \Delta H^+_{Cyt\,c^{3+}}}{(1-\alpha)(1-\delta)} \tag{13}$$

where the additional term $-\Delta H^+_{Cyt\,c^{3+}}$ accounts for the proton release from the oxidized cytochrome.

TABLE I

ELECTRON TRANSFER REACTIONS

Reaction 1 was initiated by injection of $K_3Fe(CN)_6$; all others were light-induced. A fraction, δ, (few percent) of the RCs used in reactions 5 and 6 had lost Q_B during isolation. The RCs used in reactions 2–4 were chemically depleted of Q_B. The parameter α is the pH dependent equilibrium partition coefficient between the states $Q_A^- Q_B$ and $Q_A Q_B^-$; i.e., $\alpha = [Q_A^- Q_B]/([Q_A^- Q_B] + [Q_A Q_B^-])$. Derived proton uptakes are shown in bold face.

No.	Electron-transfer reaction and observed proton uptake	Derived proton uptake	Eqns.	Figs.
1	$\text{Cyt } c^{2+} + Fe(CN)_6^{3-} \rightarrow \text{Cyt } c^{3+} + Fe(CN)_6^{4}$ $\Delta H^+_{obs} = \Delta \mathbf{H}^+_{\text{Cyt } c^{3+}}$	$\Delta \mathbf{H}^+_{\text{Cyt } c^{3+}}$	–	2
2	$DQ_A \xrightarrow{h\nu} D^+ Q_A^-$ $\Delta H^+_{obs} = \Delta \mathbf{H}^+_{D^+ Q_A^-}$	$\Delta \mathbf{H}^+_{D^+ Q_A^-}$	–	7, 8
3	$DQ_A + \text{Cyt } c^{2+} \xrightarrow{h\nu} DQ_A^- + \text{Cyt } c^{3+}$ $\Delta H^+_{obs} = \Delta \mathbf{H}^+_{DQ_A^-} + \Delta H^+_{\text{Cyt } c^{3+}}$	$\Delta \mathbf{H}^+_{DQ_A^-}$	11	3, 4
4	$DQ_A + Fe(CN)_6^{4-}/\text{Cyt } c^{2+} \xrightarrow{h\nu} DQ_A^- + Fe(CN)_6^{3-}/\text{Cyt } c^{2+}$ $\Delta H^+_{obs} = \Delta \mathbf{H}^+_{DQ_A^-}$	$\Delta \mathbf{H}^+_{DQ_A^-}$	–	5
5	$(1-\delta)\cdot DQ_A Q_B + \delta \cdot DQ_A \xrightarrow{h\nu} (1-\delta)[\alpha \cdot D^+ Q_A^- Q_B + (1-\alpha)\cdot D^+ Q_A Q_B^-] + \delta \cdot D^+ Q_A^-$ $\Delta H^+_{obs} = (1-\delta)[\alpha \cdot \Delta H^+_{D^+ Q_A^- Q_B} + (1-\alpha)\cdot \Delta \mathbf{H}^+_{D^+ Q_A Q_B^-}] + \delta \cdot \Delta H^+_{D^+ Q_A^-}$	$\Delta \mathbf{H}^+_{D^+ Q_A Q_B^-}$	12	9
6	$(1-\delta)\cdot DQ_A Q_B + \delta \cdot DQ_A + \text{Cyt } c^{2+} \xrightarrow{h\nu} (1-\delta)[\alpha \cdot DQ_A^- Q_B + (1-\alpha)\cdot DQ_A Q_B^-] + \delta \cdot DQ_A^- + \text{Cyt } c^{3+}$ $\Delta H^+_{obs} = (1-\delta)[\alpha \cdot \Delta H^+_{DQ_A^- Q_B} + (1-\alpha)\Delta \mathbf{H}^+_{DQ_A Q_B^-}] + \delta \cdot \Delta H^+_{DQ_A^-} + \Delta H^+_{\text{Cyt } c^{3+}}$	$\Delta \mathbf{H}^+_{DQ_A Q_B^-}$	13	6

Error bars shown for the data of ΔH^+_{obs} (see the Results section) represent the estimated experimental uncertainty (one S.D.). They were calculated from the estimated uncertainties associated with the measurement of the electrode-potential and the calibration of the potential in terms of proton uptake (see Materials and Methods). Error bars shown for the derived proton uptakes ($\Delta H^+_{DQ_A^-}$, $\Delta H^+_{D^-Q_AQ_B^-}$ and $\Delta H^+_{DQ_AQ_B}$) were obtained by propagating the estimated experimental uncertainties of ΔH^+_{obs}.

Experimental results

Proton release from cytochrome c^{3+}

Cytochrome c^{2+} was used as a donor in several reactions (3 and 6, Table I). The proton release associated with the oxidation of cytochrome c^{2+} had, therefore, to be determined.

Cytochrome c^{2+} was oxidized with ferricyanide (reaction 1, Table I) and the concomitant proton release was determined by measuring the voltage across the pH electrode (Fig. 2a). Subsequent addition of ferricyanide (not shown) caused no change in pH, showing that the oxidation was complete and that no artifacts were associated with the injection. The kinetics of proton release were biphasic: the characteristic time of one phase was shorter than the response time of the apparatus ($\tau_{1/e} \leq 2$ s); the time constant of the other phase was longer and pH-dependent (e.g., pH 8.1: $\tau_{1/e} = 30$ s; pH 9.1: $\tau_{1/e} = 15$ s). The extent of oxidation of the cytochrome c^{2+} by ferricyanide was checked optically at 550 nm; it was found to be greater than 99%.

The pH-dependence of the proton release is shown in Fig. 2b. The data were fitted with the model of Eqn. 4, with the parameters $\Delta H^+_{Q\to Q^-}$, pK_{iQ}, and pK_{iQ} replaced by $\Delta H^+_{cyt\,c^{3+}}$, $pK_{iCyt\,c^{3+}}$, and $pK_{iCyt\,c^{2+}}$, respectively. A good fit was obtained with three protonatable residues ($n = 3$) with values of $pK_{iCyt\,c^{2+}}$ and $pK_{iCyt\,c^{3+}}$ given in figure caption 2b. The data of Fig. 2b are in agreement with those determined in a more limited pH range by Czerlinski and Dar [37].

Proton uptake by DQ_A^-

Two methods were used to determine the proton uptake by DQ_A^- (reactions 3 and 4, Table I).

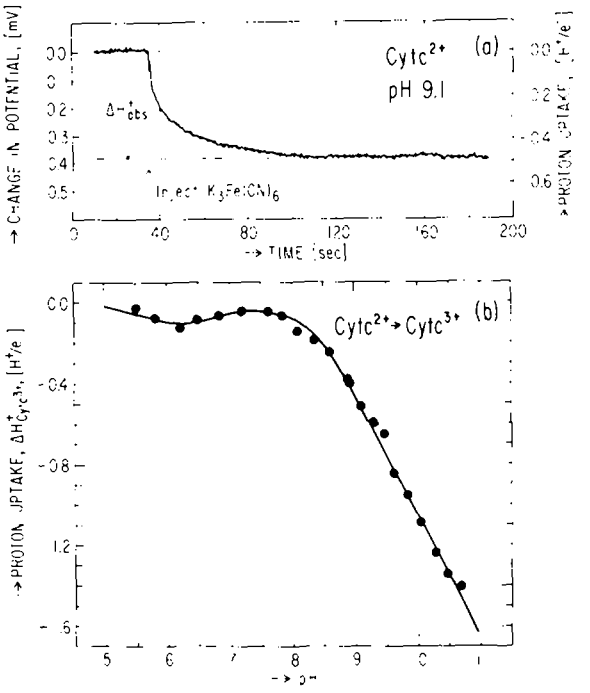

Fig. 2. Proton release associated with the oxidation of cytochrome c^{2+}. (a) Change in potential across the pH electrode following injection of ferricyanide. The change in potential was calibrated in terms of proton uptake by injecting a known amount of HCl. The concentration of cytochrome c^{2+} was determined from the change in absorption at 550 nm and the extinction coefficient ($\varepsilon^{550}_{Cyt\,c^{2+}} - \varepsilon^{550}_{Cyt\,c^{3+}}$) = 18.5 $mM^{-1}\cdot cm^{-1}$. The transient spike was caused by the injection. The value of the proton release from cytochrome c^{3+} is given by $|\Delta H^+_{obs}|$ (reaction 1, Table I). Conditions: 6 μM cytochrome c^{2+} in 0.5 mM H_2KPO_4, 0.5 mM Tris-HCl, 0.5 mM Ches, 50 mM KCl (total volume = 2.0 ml) (pH 9.1); T = 23° C. Injection: 4.0 μl 6.0 mM solution of $K_3Fe(CN)_6$. (b) pH-dependence of proton release. Dots (●) represent average of two or more measurements. Statistical errors (standard deviation of mean) ≤ radius of dot. Solid line represents best fit with Eqn. 4 for three protonatable residues ($n = 3$) having the following pK values ($pK_{iCyt\,c^{3+}}$, $pK_{iCyt\,c^{2+}}$): $i = 1$, (6.10, 6.30); $i = 2$, (9.10, ≫12); $i = 3$, (10.70, ≫12). Conditions were the same as in (a), except at pH < 8 the concentration of the buffer was reduced by a factor of 2 while keeping the KCl concentration the same.

In both, cytochrome c^{2+} reduced D^+. In method I (reaction 3, Table I), the release of protons from cytochrome c^{3+} had to be taken into account. In method II (reaction 4, Table I), ferrocyanide re-reduced cytochrome c^{3+}, eliminating the necessity of correcting for this proton release. Although method I is less accurate than method II, it is applicable over a larger pH range (5 < pH < 10.5

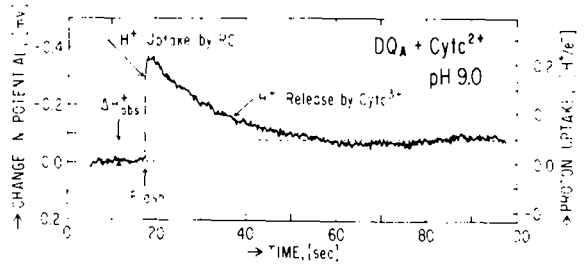

Fig. 3. Determination of observed light-induced proton uptake by DQ_A^- in the presence of cytochrome c^{2+} as donor (reaction 3, Table I). The change in potential was calibrated in terms of proton uptake by injecting a known amount of HCl. The concentration of RCs was determined from the absorption at 802 nm and the extinction coefficient $\varepsilon^{802} = 288\ mM^{-1} \cdot cm^{-1}$. The quinone content of RCs was determined as described in Materials and Methods. ΔH^+_{obs} was used to determine the proton uptake by DQ_A^- (see Fig. 4). Conditions: 3.5 μM RCs (0.78 UQ/RC), 50 μM cytochrome c^{2+} in 0.025% LDAO (w/v), 50 mM KCl (pH 9.0); $T = 23 \pm 1°$ C.

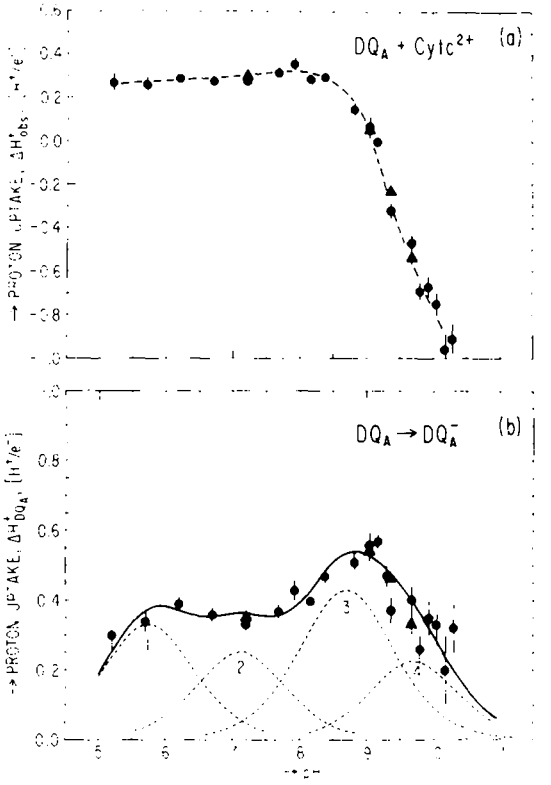

Fig. 4. Proton uptake by DQ_A^- (method I). (a) pH dependence of the observed proton uptake, ΔH^+_{obs}, determined as in Fig. 3. Conditions same as in Fig. 3, except at pH < 7.2 the concentration of LDAO was increased to 0.075% (w/v). Illumination: either continuous light (●) ($\lambda_0 = 850$ nm, $\Delta\lambda = 50$ nm, $I = 34\ mW/cm^2$) or light-flash (▲) ($\lambda_0 = 590$ nm, 0.4 μs in duration, 0.2 J per flash). (b) pH dependence of proton uptake by DQ_A^-, determined from the data in (a) and Eqn. 11 with $\Delta H^+_{Cyt\,c^{3+}}$ given by the data (solid line) in Fig. 2b. Solid line is best fit with Eqn. 4 for four protonatable residues ($n = 4$) having the following pK values (pK_{iQ_A}, $pK_{iQ_A^-}$): $i = 1$, (5.45, 6.05); $i = 2$, (6.90, 7.35); $i = 3$, (8.30, 9.10); $i = 4$, (9.50, 9.90) [§]. Dashed lines are individual contributions of residues. Error bars represent estimated statistical errors; where absent, error bars are not greater than the size of ● or ▲.

as compared to 6 < pH < 10.5) and can be used to determine the proton uptake by $DQ_AQ_B^-$. Method II, in contrast to method I, requires the use of continuous illumination (as discussed below) and is therefore not applicable to the proton uptake by $DQ_AQ_B^-$ *. The results of methods I and II were compared as shown below; they were found to be in satisfactory agreement.

Method I

DQ_A^- was generated by illuminating Q_B-depleted RCs in the presence of cytochrome c^{2+} with either continuous light or light-flashes. The proton uptake was determined from the potential across the pH electrode as shown in Fig. 3. The magnitude of the observed initial uptake (0.2 H^+/e^- at pH 9.0) corresponds to the sum of the proton uptake by DQ_A^- and the fast, unresolved, phase of the proton release by cytochrome c^{3+} (see Fig. 2a). The slower release of protons following the light-flash had a time constant characteristic of the slower phase of the proton release from cytochrome c^{3+} (e.g., pH 8.0: $\tau_{1/e} = 27 \pm 5$ s; pH 9.0: $\tau_{1/e} = 14 \pm 2$ s). The observed proton uptake was determined after steady state was reached ($t > 60$ s). A second flash (not shown) caused no change in pH, showing: (i) the absence of artifacts associated with the flash; (ii) the completion of the reaction; and (iii) the absence of a back-reac-

* Continuous illumination of DQ_AQ_B in the presence of cytochrome c^{2+} would cause two electrons to be transferred to Q_B.

§ One can view each residue in our model as a class of protonatable residues each having approx the same pK_{iQ} and pK_{iQ^-}.

tion (i.e., oxidation of Q_A^- by cytochrome c^{3+}) during the measurement.

The pH-dependence of the observed proton uptake (ΔH^+_{obs}) is shown in Fig. 4a. Measurements were limited to pH < 10.5 because of the slow reduction of D^+ by cytochrome c^{2+} at higher pH [15]. For pH > 9, the proton release from cytochrome c^{3+} is larger than the proton uptake by DQ_A^-, resulting in negative values of ΔH^+_{obs}.

The proton uptake by DQ_A^- (Fig. 4b) was determined from ΔH^+_{obs} (Fig. 4a) and Eqn. 11; the values of $\Delta H^+_{Cyt\,c^{3+}}$ were obtained from the data in Fig. 2b (solid line). The proton uptake data (Fig. 4b) were fitted with the model of Eqn. 4. A good fit was obtained for four protonatable residues ($n = 4$) with values of pK_{iQ_A} and $pK_{iQ_A^-}$ given in figure caption 4b *.

Two controls were done to check if the detergent used to solubilize the reaction centers affected the proton uptake. In one the concentration of LDAO was varied from 0.025% to 0.075% (w/v) at pH 7.0 and 9.0, and in the other LDAO was replaced with 0.040% dodecyl-β-D-maltoside (see Materials and Methods) at pH 6.2. Neither change affected the proton uptake.

Method II

In this method, DQ_A^- was generated by illuminating Q_B-depleted reaction centers in the presence of cytochrome c^{2+} with continuous light. The redox potential was buffered with ferricyanide/ferrocyanide which kept the cytochrome c^{2+} reduced, preventing it from releasing protons. Since LDAO reacts with ferricyanide, it had to be replaced by another detergent. Dodecyl-β-D-maltoside was chosen because it does not affect the proton uptake (see previous paragraph).

The determination of proton uptake is shown in Fig. 5a. The potential across the electrode following illumination shows a slow decay due to heating of the solution (see discussion at the end of this section). The value of ΔH^+_{obs} was obtained by extrapolating the potential to the time when the light was turned on (see Fig. 5a). The decay of the potential when the light was turned off is due

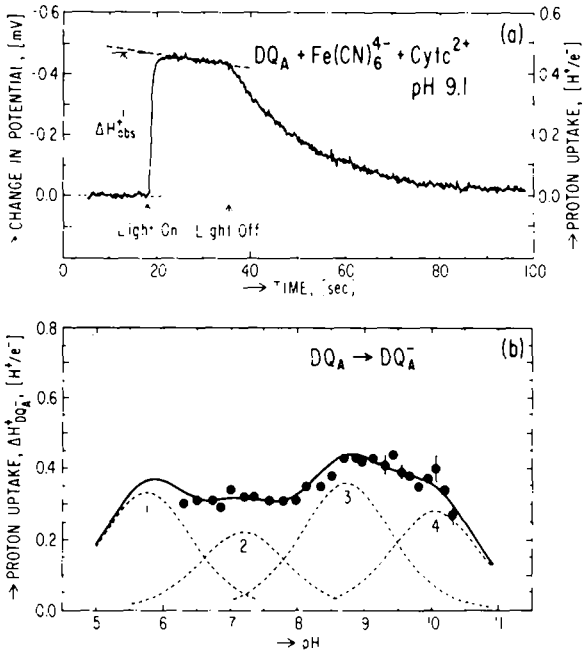

Fig. 5. Proton uptake by DQ_A^- (method II). (a) Change in electrode-potential following illumination. The oxidation of cytochrome and its concomitant release of protons was prevented by buffering the redox potential with ferricyanide/ferrocyanide at 330 mV (vs. the standard hydrogen electrode) (reaction 4, Table I). The decay after turning off the light was caused by oxidation of Q_A^- by ferricyanide. Calibration of the change in potential in terms of proton uptake same as in Fig. 3. ΔH^+_{obs} is equal to the proton uptake by DQ_A^-. Conditions (at redox-equilibrium): 3.5 μM RCs (0.78 UQ/RC), 1 μM cytochrome c^{2+}, 22 μM cytochrome c^{3+}, 1 mM $K_4Fe(CN)_6$, 30 μM $K_3Fe(CN)_6$ in 0.040% (w/v) Dodecyl-β-D-Maltoside, 50 mM KCl (pH 9.1) $T = 23 \pm 1$°C. Illumination: $\lambda_0 = 850$ nm, $\Delta\lambda = 50$ nm, $I = 10$ mW/cm². (b) pH dependence of the proton uptake by DQ_A^-. Solid line is best fit with Eqn. 4 for four protonatable residues ($n = 4$) having the following pK values (pK_{iQ_A}, $pK_{iQ_A^-}$): $i = 1$, (5.45, 6.05); $i = 2$, (7.00, 7.40); $i = 3$ (8.40, 9.05); $i = 4$, (9.80, 10.30) §. Dashed lines are individual contributions of residues. Error bars represent estimated statistical errors; where absent, error bars are not greater than radius of dot (●). Conditions: same as in (a) except that the pH-dependent midpoint potential of cytochrome c required that the total concentration of cytochrome c (i.e., [Cyt c^{2+}] + [Cyt c^{3+}]) be varied from 10 μM (pH 6) to 110 μM (pH 10) in order to maintain [Cyt c^{2+}] at 1 μM.

* One can view each residue in our model as a class of protonatable residues each having approx. the same pK_{iQ} and pK_{iQ^-}.

§ One can view each residue in our model as a class of protonatable residues each having approx. the same pK_{iQ} and pK_{iQ^-}.

to the oxidation of Q_A^- by ferricyanide [20] and the concomitant release of protons from DQ_A. The rate of oxidation increased with decreasing pH at pH < 8; this limited the measurements to pH > 6. The reaction was completely reversible; i.e., a second illumination caused a change in potential of the same magnitude as the first.

The proton uptake by DQ_A^- was obtained directly from ΔH^+_{obs} (reaction 4, Table I). Its pH dependence, shown in Fig. 5b, agrees with that determined by method I (Fig. 4b) to within 0.1 H^+/e^-. For further comparison of the two methods, the data were fitted with Eqn. 4. Four residues ($n = 4$) were again necessary to obtain a good fit *. The values of three sets of pK values (listed in caption of Fig. 5b) are in satisfactory agreement with those obtained by method I (see Fig. 4b). The values of one set (pK_{1Q_A} and $pK_{1Q_A^-}$) could not be determined because of the lack of data at pH < 6; they were assumed to be the same as obtained by method I.

In the analysis of the data we assumed that: (i) D was fully reduced prior to illumination; (ii) cytochrome c^{2+} was kept fully reduced at equilibrium; and (iii) Q_A^- was not oxidized by ferricyanide during illumination. To determine the validity of these assumptions the following controls were performed under conditions as described in Fig. 5a except for the addition of 10 mM buffer (Pipes, Tris-HCl or Ches depending on pH): (i) The extent of reduction of D was assayed optically at 865 nm and was found to be more than 99% at 6.2 < pH < 10.2. (ii) The reduction of cytochrome c^{2+} at equilibrium was measured optically at 550 nm. A net oxidation of up to 0.02 cytochrome c^{2+} per electron transferred to Q_A occurred at 6.2 < pH < 10.2. Note that if cytochrome c^{2+} had been oxidized, Fig. 5a would have shown a decay in the potential after the light was turned on as observed in Fig. 3. (iii) The rate of formation of DQ_A^-, k_f, was determined from the kinetics of transient absorption changes at 550 nm. These changes are caused by the formation and subsequent decay of D^+ and therefore monitor the reaction $DQ_A \rightarrow D^+Q_A^- \rightarrow DQ_A^-$. The decay rate of DQ_A^-, k_d, was obtained from the decay of the proton uptake when the light was turned off. The ratio k_f/k_d was more than 100 at 6.2 < pH < 10.2, indicating more than 99% formation of DQ_A^- at equilibrium. The decay time $1/k_d$ was faster than could be measured at pH < 6.2 ($\tau_{1/e}$ < 2 s). The kinetics of the absorption changes also showed that under these conditions the characteristic time of reduction of D^+ by cytochrome c^{2+} varied from $\tau_{1/e}$ = 25 ms at pH 6.2 to $\tau_{1/e}$ = 200 ms at pH 10.0. These times are too long compared to the characteristic time of charge recombination $D^+Q_A^- \rightarrow DQ_A$ in the dark [15] ($\tau_{1/e}$ = 100 ms at 6 < pH < 10.5) to obtain charge separation in all the RCs with a light-flash *. We therefore used only continuous illumination in method II. The reduction of D^+ is also too slow to obtain complete charge separation in RCs with approx. two quinones with a light-flash because these RCs form a significant amount of Q_A^- (see reaction 6, Table I).

As mentioned above, the slow decay of the electrode potential when the light was turned on is believed to be due to heating of the solution. This was shown by the following controls. (i) Illumination under the same conditions as in Fig. 5a, except for the absence of RCs caused no change in potential. Heating was absent in this case because the solution did not absorb light at 850 nm. (ii) Illumination at approx. 2500 nm (Corning 5-59 and 7-56 filters; other conditions same as in Fig. 9), where RCs are not excited but light is absorbed by the water causing heating, caused a slow decay similar to that observed in Figs. 5a and 7. (iii) The value of the slope of the slow decay in time was directly proportional to the intensity, I, of the incident light at 1 mW/cm^2 < I < 40 mW/cm^2 (other conditions same as in Fig. 5a). In contrast, ΔH^+_{obs} and therefore the extent of charge separation DQ_A^- did not vary with I. The amount of heating was observed to be proportional to I as expected.

* One can view each residue in our model as a class of protonatable residues each having the same $pK_{/Q}$ and $pK_{/Q^-}$.

* The reduction of D^+ was fast enough in method I to obtain complete charge separation with a light-flash because a higher concentration of cytochrome c^{2+} was used. A lower concentration had to be used in method II in order to prevent a significant amount of cytochrome c^{2+} from being oxidized.

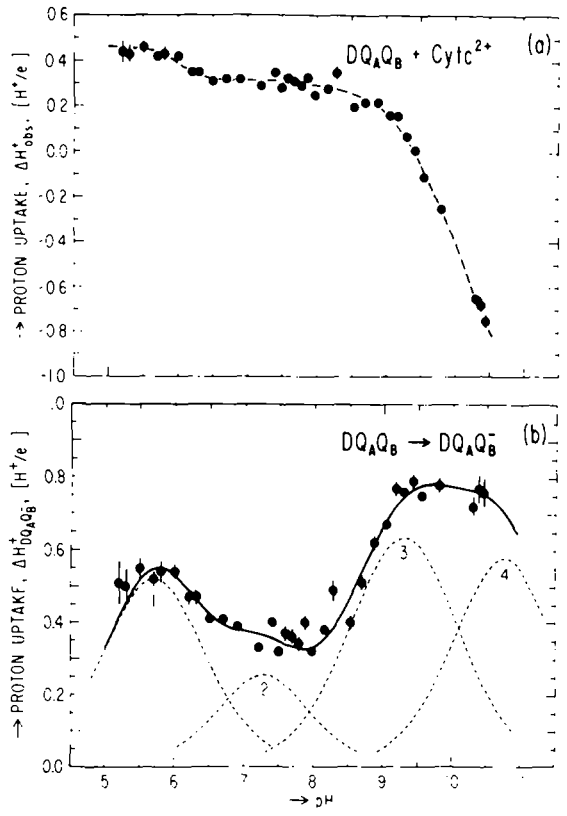

Fig. 6. Proton uptake by $DQ_AQ_B^-$. (a) pH dependence of the observed proton uptake, ΔH^+_{obs}, with cytochrome c^{2+} as donor (reaction 6, Table I). ΔH^+_{obs} was determined from the change in potential as shown in Fig. 3 for DQ_A^-. Conditions: 3.5 μM RCs (1.92 UQ/RC), 50 μM cytochrome c^{2+} in 50 mM KCl, 0.025% (w/v) LDAO (pH > 7.2) or 0.075% LDAO (pH < 7.2); $T = 23 \pm 1$°C. Illumination: light-flash ($\lambda_0 = 590$ nm). (b) pH dependence of proton uptake by $DQ_AQ_B^-$, obtained from data of (a) and Eqn. 13 as described in text. Solid line is best fit with Eqn. 4 for four protonatable residues ($n = 4$) having the following pK values (pK_{iQ_B}, p$K_{iQ_B^-}$): $i = 1$, (5.20, 6.20); $i = 2$, (7.05, 7.50); $i = 3$, (8.65, 9.95); $i = 4$, (10.20, 11.35) §. Dashed lines are individual contributions of residues. Error bars represent estimated statistical errors; where absent, error bars are not larger than radius of dot (●).

Proton uptake by $DQ_AQ_B^-$

The procedure for observing proton uptake by $DQ_AQ_B^-$ was the same as shown in Fig. 3 for DQ_A^- (method I) except that RCs with approx. two quinones were used (reaction 6, Table I). The pH dependence of ΔH^+_{obs} is shown in Fig. 6a. The proton release from cytochrome c^{3+} exceeds the proton uptake by $DQ_AQ_B^-$ for pH > 9, resulting in negative values of ΔH^+_{obs}. The proton uptake by $DQ_AQ_B^-$ was obtained from ΔH^+_{obs} and Eqn. 13. Values of $\Delta H^+_{Cyt\,c^{3+}}$ and $\Delta H^+_{DQ_A}$ were obtained from the data (solid lines) in Figs. 2b and 4b, and δ was determined to be 0.08 (see Materials and Methods). Values of α were obtained from the relation [15]:

$$\alpha = \frac{1}{1+\exp(-\Delta G^0/kT)}$$

$$\Delta G^0 = -67\ \text{meV} - kT \ln \frac{1+10^{\text{pH}-11.3}}{1+10^{\text{pH}-9.8}} \qquad (14)$$

The proton uptake by $DQ_AQ_B^-$ was fitted (solid line, Fig. 6b) with Eqn. 4 assuming four protonatable residues ($n = 4$) with values of pK_{iQ_B} and p$K_{iQ_B^-}$ given in figure caption 6b *. Note that the dominant terms in Eqn. 13 are ΔH^+_{obs} and $\Delta H^+_{Cyt\,c^{3+}}$; if α and δ are set to zero, the derived proton uptake differs from that in Fig. 6b by only 5% at pH < 9.0 and 23% at pH = 10.4.

The following controls were performed. (i) To check whether the flash resulted in complete charge separation, two flashes were given to Q_B-depleted RCs in the presence of cytochrome c^{2+}. The absence of a measurable change in pH following the second flash showed that more than 97% of the RCs were excited. (ii) Whether or not cytochrome c^{3+} re-oxidized Q_A^- or Q_B^- during the measurement was checked optically at 550 nm (at pH = 8.0 and 10.0); no re-oxidation was detected (limit of detection = 3%). (iii) Possible effects of the detergent LDAO were checked by varying its concentration from 0.075% to 0.15% (w/v; pH 6.0) and from 0.025% to 0.075% (pH 7.5 and 9.2); the observed proton uptake was unchanged. (iv) Possible irreversible changes in the reaction centers at extreme pH were checked by adjusting the pH to either 5.0 or 11.0 for 5 min then returning it to 7.5 and measuring the proton uptake. Complete reversibility was observed.

§ One can view each residue in our model as a class of protonatable residues each having the same pK_{iQ} and pK_{iQ^-}.

* One can view each residue in our model as a class of protonatable residues each having the same pK_{iQ} and pK_{iQ^-}.

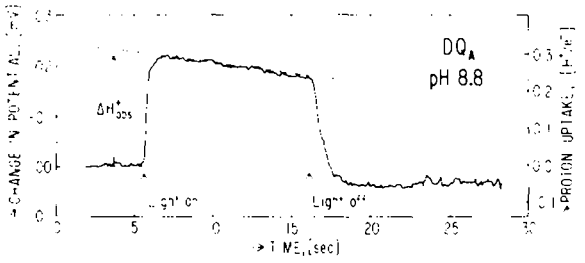

Fig. 7. Determination of proton uptake by $D^+Q_A^-$ (reaction 2, Table I). The change in potential was calibrated in terms of proton uptake as described in Fig. 3, except that the degree of light-saturation of the state $D^+Q_A^-$ (94%) had to be taken into account (see text). ΔH^+_{obs} is equal to the proton uptake by $D^+Q_A^-$. Conditions: 3.5 μM RCs (0.96 UQ/RC) in 0.025% (w/v) LDAO, 50 mM KCl (pH 8.8); $T = 23 \pm 1°$ C. Illumination: $\lambda_0 = 850$ nm, $\Delta\lambda = 50$ nm, $I = 65$ mW/cm^2.

Proton uptake by $D^+Q_A^-$ and $D^+Q_AQ_B^-$

The proton uptake by $D^+Q_A^-$ was determined by illuminating Q_B-depleted reaction centers with continuous light (reaction 2, Table I). Data at pH 8.8 are shown in Fig. 7. When the light was turned off, $D^+Q_A^-$ decayed via charge recombination resulting in the release of protons. The slope during illumination and the resulting offset were caused by heating as discussed previously. A second illumination (not shown) caused a change in potential of the same magnitude as the first, showing that the reaction centers were not damaged by light. The proton uptake (right ordinate in Fig. 7) includes a correction (few percent) due to the lack of complete charge separation $D^+Q_A^-$, as discussed below.

The pH dependence of the proton uptake is shown in Fig. 8. There is a striking difference

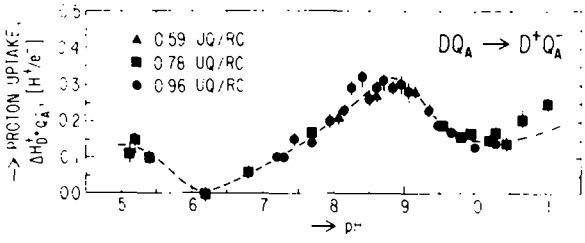

Fig. 8. pH dependence of proton uptake by $D^+Q_A^-$, determined as shown in Fig. 7. Error bars represent estimated statistical errors; where absent, error bars are not larger than size of ● or ■. Conditions are the same as in Fig. 7, except the concentration of LDAO was increased to 0.075% (w/v) at pH < 7.2 and some RCs contained 0.59 or 0.78 quinones as indicated. UQ, ubiquinone.

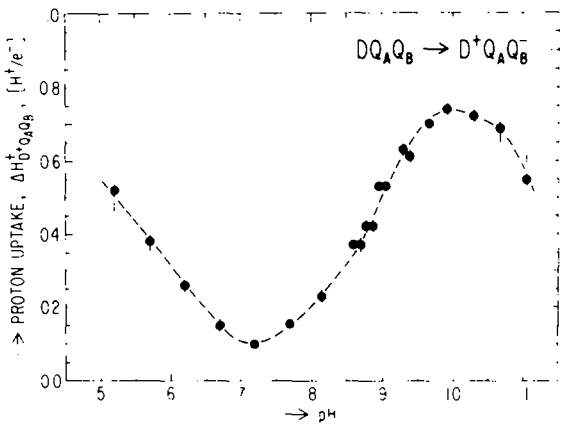

Fig. 9. pH dependence of the proton uptake by $D^+Q_AQ_B^-$, determined from the observed proton uptake, ΔH^+_{obs}, of reaction 5 (Table I) and Eqn. 12 as described in text. ΔH^+_{obs} (not shown) was determined as shown in Fig. 7 for $D^+Q_A^-$. Error bars represent estimated statistical errors; where absent, error bars are not larger than radius of dot (●). Conditions are the same as in Fig. 7, except that the reaction centers contained 1.92 UQ/RC and the concentration of LDAO was 0.075% (w/v) at pH < 7.2.

between these data and those for DQ_A^- (Figs. 4b and 5b), particularly at low pH where the value of the proton uptake by DQ_A^- is as much as 0.4 H^+/e^- larger than that by $D^+Q_A^-$. This is due to proton release from D^+ as discussed in the next section.

The procedure for observing proton uptake by $D^+Q_AQ_B^-$ (reaction 5, Table I) was the same as shown in Fig. 7 for $D^+Q_A^-$ except that RCs with approx. two quinones were used. The proton uptake by $D^+Q_AQ_B^-$ was determined from ΔH^+_{obs} and Eqn. 12. Values of $\Delta H^+_{D^+Q_A^-}$ were obtained from the dashed curve drawn through the data of Fig. 8, δ was determined to be 0.08 (see Materials and Methods), and α was obtained from Eqn. 14. The proton uptake by $D^+Q_AQ_B^-$ (Fig. 9) is less than that by $DQ_AQ_B^-$ (Fig. 6b) due to proton release from D^+.

Continuous illumination was necessary because the charge recombination of $D^+Q_A^-$ and $D^+Q_AQ_B^-$ is faster than the response time of the electrode, precluding detection of flash-induced protonation (at pH 8, $\tau_{1/e} = 1/k_d = 0.1$ and 1 s for $D^+Q_A^-$ and $D^+Q_AQ_B^-$, respectively [15]). The formation rate, k_f, of the state $D^+Q_A^-$ or $D^+Q_AQ_B^-$ is proportional to the intensity of the illumination [35]. In

order to obtain charge separation in all RCs (light-saturation), the intensity of the light must be sufficiently high to ensure that $k_f \gg k_d$. However, at high light intensities heating of the sample occurred. We chose a light intensity $I = 65$ mW/cm^2, which represented a compromise between lightsaturation and heating. The degree of saturation was determined as described by McElroy et al. [35]. At $I = 65$ mW/cm^2 and pH 8.0 it was 0.94 and 0.99 for the states $D^+Q_A^-$ and $D^+Q_AQ_B^-$, respectively. The degree of saturation was extrapolated to other pH from the known pH dependence of k_d [15]. It varied less than 0.02 and 0.05 for $D^+Q_A^-$ and $D^+Q_AQ_B^-$, respectively, at $6 < pH < 11$.

Proton release from D^+

The proton uptake by $D^+Q_A^-$ and $D^+Q_AQ_B^-$ (Figs. 8 and 9) is less than that by DQ_A^- and $DQ_AQ_B^-$ (Figs. 4b, 5b and 6b). This decrease in net proton uptake has been ascribed to a release of protons from D^+ [19,20]. The difference $\Delta H^-_{D^+Q_A^-} - \Delta H^+_{DQ_A^-}$, obtained from the average of the data of Figs. 4b and 5b (dots) and the data of Fig. 8 (dashed line), gives the proton release associated with the reaction $DQ_A^- \rightarrow D^+Q_A^-$ and is plotted in Fig. 10 (○). The difference $\Delta H^+_{D^+Q_AQ_B^-} - \Delta H^+_{DQ_AQ_B^-}$, obtained from the data of Figs. 6b (dots) and 9 (dashed line), gives the proton release associated with the reaction $DQ_AQ_B^- \rightarrow D^+Q_AQ_B^-$ and is also plotted in Fig. 10 (△). The two curves (○ and △) agree within the experimental uncertainty at $7 < pH < 9$ but differ by approx. 0.1 H^+/e^- at $pH < 7$ and $pH > 9$. It is not clear at present whether this relatively small difference of approx. 0.1 H^+/e^- is real or is due to an unknown systematic error. A real difference would mean that the proton release from D^+ is affected by the redox state of the quinones. This possibility is discussed in a later section.

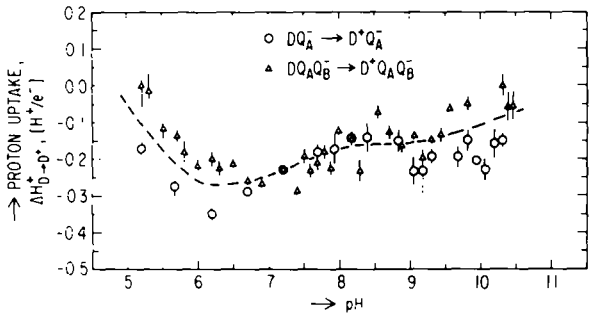

Fig. 10. Proton release from D^+. The difference $\Delta H^+_{D^+Q_A^-} - \Delta H^+_{DQ_A^-}$ (○) was obtained from the average of the data of Figs. 4b and 5b (dots) and the data of Fig. 8 (dashed line). The difference $\Delta H^+_{D^+Q_AQ_B^-} - \Delta H^+_{DQ_AQ_B^-}$ (△) was obtained from the data of Figs. 6b (dots) and 9 (dashed line).

Free-energy changes associated with the reduction of Q_A and Q_B

The pH dependence of the free-energy changes, $\Delta G^0_{Q \rightarrow Q^-}$, accompanying the reduction of Q_A and Q_B was determined by integrating the proton uptake by DQ_A^- (Fig. 5b) and $DQ_AQ_B^-$ (Fig. 6b), respectively (see Eqn. 10). The integration was performed by summing the areas under the line segments connecting consecutive data points. The integration constants were chosen to make the difference $\Delta G^0_{Q_B \rightarrow Q_B} - \Delta G^0_{Q_A \rightarrow Q_A^-}$ at pH 7.0 equal

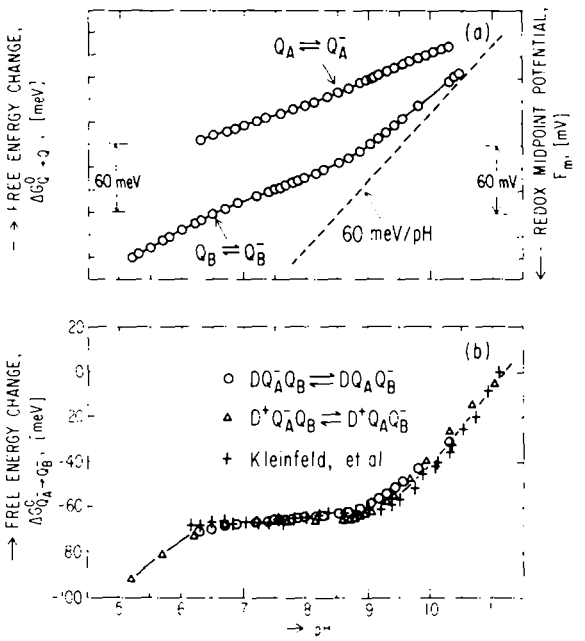

Fig. 11. Free-energy differences between quinone states. (a) Free-energy differences (redox midpoint potentials) between the states Q_A and Q_A^- and between the states Q_B and Q_B^-, calculated by integrating the proton uptake by DQ_A^- (Fig. 5b) and $DQ_AQ_B^-$ (Fig. 6b) as described in text. Absolute values of free energy differences were not determined. (b) Free energy differences between the states $D^+Q_A^-Q_B$ and $D^+Q_AQ_B^-$ (△) obtained by integrating the data of Figs. 8 and 9 and between the states $DQ_A^-Q_B$ and $DQ_AQ_B^-$ (○) obtained from (a) and Eqn. 15. The data of Kleinfeld et al. [15] for the free energy between $D^+Q_A^-Q_B$ and $D^+Q_AQ_B^-$ (+) are shown for comparison.

to the value measured by Kleinfeld et al. [15] as discussed below. The results are shown in Fig. 11a. The absolute values of the free-energy changes are not indicated because only the difference between the integration constants was determined. The redox midpoint potential, E_m (the negative of the free-energy change), of Q_A decreases with increasing pH by approx. 20 mV/pH at $6 < pH <$ 10. For Q_B a decrease of approx. 20 mV/pH at $6 < pH < 9$ and approx. 40 mV/pH at $pH > 9$ and $pH < 6$ was obtained.

The free energy, $\Delta G^0_{Q_A^- \rightarrow Q_B^-}$, between the states $DQ_A^-Q_B$ and $DQ_AQ_B^-$ was calculated from the difference in the free energies; i.e.,

$$\Delta G^0_{Q_A^- \rightarrow Q_B} = \Delta G^0_{Q_B \rightarrow Q_B^-} - \Delta G^0_{Q_A \rightarrow Q_A^-} = E_{m(Q_A)} - E_{m(Q_B)} \tag{15}$$

The pH dependence is shown in Fig. 11b (○). The free energy between the states $D^+Q_A^-Q_B$ and $D^+Q_AQ_B^-$ was obtained in a similar way (from Figs. 8 and 9) and is also plotted in Fig. 11b (△). There is no difference, within experimental error, between the two curves (○ and △), in agreement with the results of Kleinfeld et al. [15]. For comparison, the data of Kleinfeld et al. [15] are also plotted in Fig. 11b (+). The integration constant in Eqn. 10 was chosen to set the three sets of data equal to each other at pH 7. The pH dependences of the three curves are in good agreement, differing at most by 5 meV throughout the pH range.

Conclusions and Discussion

Proton uptake by DQ_A^- and $DQ_AQ_B^-$

We have investigated the proton uptake associated with the reduction of Q_A and Q_B in RCs from *Rb. sphaeroides* R-26. We found the proton uptake by DQ_A^- (Figs. 4b and 5b) to be pH-dependent with a maximum value of approx. 0.5 H^+/e^-, at pH 9. The proton uptake by $DQ_AQ_B^-$ (Fig. 6b) is also pH dependent with a maximum value of approx. 0.8 H^+/e^-, at pH 9.5–10.5.

Cogdell et al. [16] reported that an uptake of 0.25–0.30 H^+/e^- accompanies the formation of DQ_A^- in RCs from *Rb sphaeroides* at pH 7.5, in good agreement with our results §. More recently, Maroti and Wraight [19] reported values of approx. 0.5 H^+/e^- at pH 8–10 and approx. 0.7 H^+/e^- at pH 6–7 for the proton uptake by DQ_A^- in RCs from *Rb. sphaeroides*. For $DQ_AQ_B^-$, they observed an uptake of approx. 0.8 H^+/e^- at $5 <$ $pH < 10$ *. Our data are in agreement with theirs at $pH > 8$, but agree only within a factor of approx. 2 at lower pH. The reason for this discrepancy is not understood at present.

The optical and EPR spectra of DQ_A^- and $DQ_AQ_B^-$ indicate that neither Q_A^- nor Q_B^- is protonated directly [26–29] **, suggesting that the protons are taken up by protonatable amino acid residues of the RC protein [14,19,20]. We fitted the pH-dependence of the proton uptake of either DQ_A^- or $DQ_AQ_B^-$ empirically by assuming four non-interacting protonatable residues and using their pK values (pK_{iQ} and pK_{iQ^-}) as adjustable parameters (Figs. 4b, 5b and 6b). It should be emphasized, however, that the assumption of non-interacting residues oversimplifies the real situation. Furthermore, the fit is not unique; a larger number of protonatable residues would improve the fit. Indeed, as we shall point out in a later section, the number of residues contributing to the proton uptake is believed to be much larger than four ***. However, we believe that the accuracy of the data at present does not warrant a more complicated fitting procedure. It should be noted that these protonation schemes are qualitatively similar to that proposed for the Bohr effect in hemoglobin, in which protons are taken up by several residues whose pKs are shifted when O_2 dissociates (see, e.g., Ref. 39).

§ They did not correct their data for the proton release from cytochrome c^{3+} (approx. 0.05 H^+/e^- at pH 7.5; see Fig. 2b and Eqn. 11).

* Maróti and Wraight originally reported a value of 1.0 H^+/e [20], but now believe that it is closer to 0.8 H^+/e^- (C. Wraight, personal communication).

** The spectra were taken at pH 7.5–8.0 [26–29]. Ubisemiquinone in isopropanol/acetone has a pK of 5.9 and in water would be expected to have a pK of approx. 5 [38]. Evidence that neither Q_A nor Q_B protonates directly at $pH > 5$ is provided by the data of Figs. 4b and 6b, which correspond to the indirect protonation model of Fig. 1b.

*** One can view each residue in our model as a class of protonatable residues each having approx. the same pK_{iQ} and pK_{iQ^-}.

Proton uptake by $D^+Q_A^-$ and $D^+Q_AQ_B^-$

The proton uptake by $D^+Q_A^-$ and $D^+Q_AQ_B^-$ is less than that by DQ_A^- and $DQ_AQ_B^-$. The difference, attributed to the release of protons from D^+ [19,20], is shown in Fig. 10. Since we observe net proton uptake by $D^+Q_A^-$ and $D^+Q_AQ_B^-$, the average interaction of protonatable residues with Q_A^- or Q_B^- is stronger than with D^+.

The pH dependence of the free-energy difference between $D^+Q_A^-$ and DQ_A has been obtained by integrating the proton uptake by $D^+Q_A^-$, i.e., using Eqn. 10 with $\Delta H^+_{Q\to Q^-}$ replaced by $\Delta H^+_{D^+Q_A^-}$ [40,41]. These results have been used to explain the pH dependence of the charge recombination kinetics of $D^+Q_A^-$ [40,41]. The free energy between $D^+Q_A^-$ and DQ_A has been recently obtained in an elegant way from an analysis of the delayed fluorescence yield [42,43].

pH dependence of the redox potentials of Q_A and Q_B

Redox titrations of Q_A in chromatophores of *Rb. sphaeroides* [21–23] and isolated RCs from *Rb. sphaeroides* incorporated into liposomes [24] showed a pH-dependent midpoint potential at $5 < pH < 10$, whose slope had a value of -60 mV per pH. As discussed in the section on theoretical models, this value corresponds to an uptake of 1 H^+/e^- *. This is in conflict with the observed proton uptake in isolated RCs (Figs. 4b and 5b) and thus warrants a more detailed discussion.

In this work, we determined the pH dependence of the midpoint potentials of Q_A and Q_B in isolated RCs (Fig. 11a) by integrating the proton uptake by DQ_A^- and $DQ_AQ_B^-$ (see Eqn. 10). This procedure is model-independent and is therefore not affected by any assumptions about the number of protonatable residues or whether they interact. The midpoint potential of Q_A ($E_{m(Q_A)}$) was found to be proportional to pH with a slope of approx. -20 mV per pH. Thus, the value of the slope of $E_{m(Q_A)}$ in isolated RCs is a factor of approx. 3 less than that determined from redox titrations of chromatophores or RCs incorporated into liposomes **. Dutton et al. [21] found even a weaker pH dependence of $E_{m(Q_A)}$ in isolated RCs from *Rb. sphaeroides*. Their redox titrations of isolated RCs indicate that $E_{m(Q_A)}$ decreases less than 25 mV from pH 5 to 9. A similar difference between isolated and membrane-bound RCs (i.e., in chromatophores) has been reported for the bacterium Erythrobacter species OCH 114 [44,45].

The midpoint potential of Q_B has been investigated to a lesser extent. We found in this work a slope for the pH dependence of $E_{m(Q_B)}$ of approx. -20 mV/pH at $6 < pH < 9$ and approx. -40 mV/pH at $pH < 6$ and $pH > 9$. Rutherford and Evans [25] reported a change in $E_{m(Q_B)}$ in chromatophores from *Rb. sphaeroides* of 90 mV between pH 8 and pH 10. We found in isolated RCs a change of approx. 70 mV in the same pH range, which agrees within approx. 30% with the data of Rutherford and Evans [25].

The serious discrepancy between the pH dependence of $E_{m(Q_A)}$ in isolated and membrane-bound RCs is of concern. Are the differences real or are they caused by some artifacts of the measurement? It is possible that the results of the redox titrations are affected by the poor equilibration between Q_A and the redox dyes that are used [24]. A determination of the pH dependence of $E_{m(Q_A)}$ from the yield of the delayed fluorescence (see, e.g., Refs. 42 and 43) may help to resolve this question. The advantage of this method is that it does not rely on the equilibration of redox dyes.

If the differences discussed above should stand up to further scrutiny, can one understand the strong effect of the membrane on the pH dependence of $E_{m(Q_A)}$? The steeper slope of $E_{m(Q_A)}$ vs. pH in membrane-bound RCs indicates a stronger interaction between Q_A^- and the protonatable residues. Such an increase in the interaction energy could be caused by a decrease in the effective dielectric constant by the membrane. Modeling the electrostatic interaction in isolated and mem-

* Figs. 1d–1f show this relation for the case in which the protons are taken up by one group. A slope of -60 mV/pH is also expected when several groups have a combined proton uptake of 1 H^+/e^- (see Eqn. 10).

** It should be noted that in this work Q_A was photo-reduced whereas in the redox titrations Q_A was chemically reduced. Although the proton uptake is not expected to depend on the method of reduction, this point needs to be investigated further.

brane-bound RCs along the lines discussed in a later section may shed some light on this question.

pH-dependence of the free energy between $Q_A^- Q_B$ and $Q_A Q_B^-$

The difference in free energy, $\Delta G^0_{Q_A^- \to Q_B^-}$, between $Q_A^- Q_B$ and $Q_A Q_B^-$ was obtained in isolated RCs by two independent methods. In this work, we integrated the proton uptake over pH and obtained $E_{m(Q_A)}$ and $E_{m(Q_B)}$ (Eqn. 10, Fig. 11a). $\Delta G^0_{Q_A^- \to Q_B^-}$ was then obtained from the difference $E_{m(Q_A)} - E_{m(Q_B)}$ (Fig. 11b). In the work of Kleinfeld et al. [15] the difference in free energy was obtained from the pH dependence of the kinetics of charge recombination in $D^+ Q_A^-$ and $D^+ Q_A Q_B^-$. The data from the two sets of experiments are in good agreement as shown in Fig. 11b *. We have also shown that the pH-dependence of the free-energy difference between $DQ_A^- Q_B$ and $DQ_A Q_B^-$ is the same as between $D^+ Q_A^- Q_B$ and $D^+ Q_A Q_B^-$ (Fig. 11b).

In the experiments of Kleinfeld et al. [15], only the differences in free energy were measured. Therefore, the individual energies $E_{m(Q_A)}$ and $E_{m(Q_B)}$ could be deduced only with the aid of a particular model. Kleinfeld et al. [15] chose for their model the results obtained with chromatophores, which, as discussed in the last section, differ from those obtained with isolated RCs. Consequently, the pH dependences of the individual free energies that they reported (Fig. 8 of Ref. 15) differ from those obtained in this work (Fig. 11a). This does not affect the other conclusions reached in their work [15].

The free-energy difference $\Delta G^0_{Q_A^- \to Q_B^-}$ is important in understanding the electron transfer from Q_A to Q_B; its sign determines the direction of electron flow. For $\Delta G^0_{Q_A^- \to Q_B^-} < 0$, transfer to Q_B is favored. This corresponds to the situation at physiological pH (pH < 9) (see Fig. 11b). At higher pH, electron transfer to Q_B becomes energetically less favorable. This increase in $\Delta G^0_{Q_A^- \to Q_B^-}$ at pH > 9 arises because the slope of $E_{m(Q_B)}$ is steeper than that of $E_{m(Q_A)}$ in this pH region (see Fig. 11a and Eqn. 15). This steeper slope corresponds to a larger proton uptake, or, equivalently, to larger pK shifts of the protonatable residues (compare Figs. 4b or 5b with 6b). It shows that the charges of the protonatable residues interact more strongly with Q_B^- than Q_A^-. This preferential interaction of bound protons with Q_B^- provides the driving force for the forward electron transfer.

pH-dependence of the redox potential of D

The average of the pH dependences of the midpoint potentials of the $DQ_A^-/D^+Q_A^-$ and $DQ_AQ_B^-/D^+Q_AQ_B^-$ couples was calculated by integrating the data (dashed line) of Fig. 10 (see Eqn. 10). The potential was approximately proportional to pH with a slope of approx. −11 mV/pH. This slope is in fair agreement with that of approx. −7 mV/pH for the $DQ_AQ_B/D^+Q_AQ_B$ couple determined by redox titrations of chromatophores of *Rb. sphaeroides* at $5 < pH < 10$ [46]. An interaction of Q_A^-, Q_B^- and D^+ with some of the same protonatable residues as discussed in a later section would make the potential of D dependent on the redox state of Q_A and Q_B. This may cause a difference between the potentials of the $DQ_AQ_B/D^+Q_AQ_B$, $DQ_A^-/D^+Q_A^-$ and $DQ_AQ_B^-/D^+Q_AQ_B^-$ couples.

On the identification of the residues involved in proton uptake

The seven amino acids that have protonatable side chains are: Glu (4.5); Asp (4.5); His (6.8); Cys (8.7); Tyr (9.8); Lys (10.1) and Arg (12.5), where the numbers in parenthesis represent their typical pK values in proteins [47]. The position of the residues in the RC from *Rb. sphaeroides* is known from the primary [4–6] and three-dimensional structure [7,8]. In order to inquire about the contribution of specific residues to the observed proton uptake, we need to model their interactions with Q_A^-, Q_B^- and D^+. The interactions can occur by two mechanisms: (i) a direct electrostatic interaction between Q_A^-, Q_B^- or D^+ and the charge of the protonatable residue, (ii) a conformational change, associated with the formation of Q_A^-, Q_B^- or D^+, that alters the electrostatic interactions between protonatable residues, thereby affecting

* Our data and those of Kleinfeld et al. [15] are not completely independent, since we used the values of α determined in Ref. 15 (Eqn. 14). However, as discussed in the experimental section, the proton uptake is relatively insensitive to the values of α. Consequently, one can consider the two sets of measurements as being effectively independent.

the pKs. We assume mechanism (i) to be the dominant cause of proton uptake. We shall focus on Q_A^- and Q_B^- although the general discussion applies also to D^+.

We model the direct electrostatic interaction energy (ϕ) with Coulomb's law as has been done for other proteins [48,49]; i.e.,

$$\phi = \frac{e^2}{\epsilon r} \tag{16}$$

where e is the electronic charge, r the distance between charges, and ϵ the dielectric constant. It is difficult to calculate the dielectric constant from first principles. We shall use, therefore, the empirical, distance-dependent expression of Warshel et al. [50]:

$$\epsilon = 1 + 60(1 - e^{-0.1r}) \tag{17}$$

where r is in ångströms. Expression 17 is based on the experimental determination of ϕ vs. r (extrapolated to zero ionic strength) for several proteins in the range of 5 Å $< r <$ 20 Å *. Thus ϵ varies from 25 at $r = 5$ Å to 53 at $r = 20$ Å. The normalized interaction energy, $\phi/2.3kT$, between Q_A^- or Q_B^- and a charged residue at a distance r is plotted in Fig. 12. This energy would correspond to the shift in pK (i.e., $pK_{iQ^-} - pK_{iQ}$) of the residue if we neglect its interaction with all other residues **. We shall neglect these interactions and use the simplified model to estimate the contributions of the different residues. The limitations and consequences of this assumption will be discussed later.

We start with the residues closest to Q_B. The distances quoted were measured from the center of the ring of the quinone to the protonatable atoms using the coordinates of the crystal structure [7,8]. Three carboxyl groups, on residues Glu L212, Glu M232, and Asp L213, are approx. 7 Å from Q_B (approx. 19 Å from Q_A). These groups would normally be expected to take up protons at

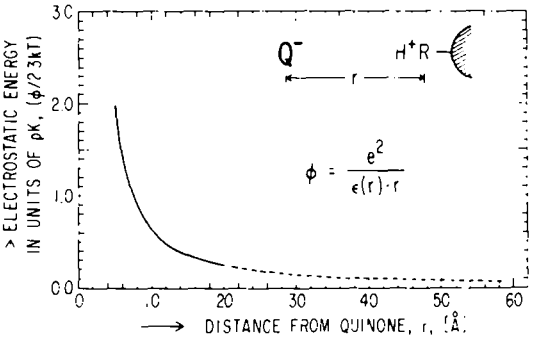

Fig. 12. Theoretical electrostatic interaction energy between two charges in the reaction center, e.g., Q^- and H^+. The dielectric constant $\epsilon(r)$ was obtained from Eqn. 17. Solid part of curve represents region of r for which Eqns. 16 and 17 have been experimentally verified in other proteins [50].

pH ≈ 5 but would be unprotonated at pH > 7. However, a theoretical analysis of the effect of protein charges on the redox potentials of Q_A and Q_B led to the suggestion that these carboxyl groups must be protonated at physiological pH (pH 7–8) in order for an electron to transfer to Q_B [51]. It is interesting that the proposed protonation of these residues to facilitate electron transfer is consistent with the stabilization of Q_B^- by protonation discussed in this work. The model (Fig. 12) predicts pK shifts of approx. 1 unit ($r = 7$ Å) for these residues. This is similar to the values of three of the pK shifts determined empirically from the proton uptake data in Fig. 6b. However, an analysis presented below indicates that other, more distant, residues may also be involved. Site-specific mutagenesis of these residues (i.e., to their non-protonatable analogs Asn and Gln) as well as calculation of their intrinsic pK values [52] should help to quantitate their contributions.

The remaining amino acids with protonatable side chains that are near Q_A or Q_B (less than 10 Å away) are the Fe^{2+} ligands, His M219, His M266, His L190, His L230 and Glu M234, and Tyr H40, which is approx. 6 Å from Q_A (approx. 20 Å from Q_B). The ligands are not expected to be protonated while coordinated to Fe^{2+}. Tyr H40 is predicted by the model (Fig. 12) to have a pK shift of approx. 1.4 ($r = 6$ Å). The value of the pK shift determined empirically (Figs. 4b and 5b) for the residue that contributes to the observed proton uptake by DQ_A^- at pH ≈ 10 is 0.5. The poor agreement between the predicted and observed

* Warshel et al. [50] indicated that the expression of Eqn. 17 had a relative uncertainty of 50% when applied to an arbitrary protein.

** Each of the non-interacting residues stabilizes Q^- by an amount equal to the difference between Eqns. 7 and 8; i.e., $\phi = 2.3\ kT\ [pK_{iQ^-} - pK_{iQ}]$.

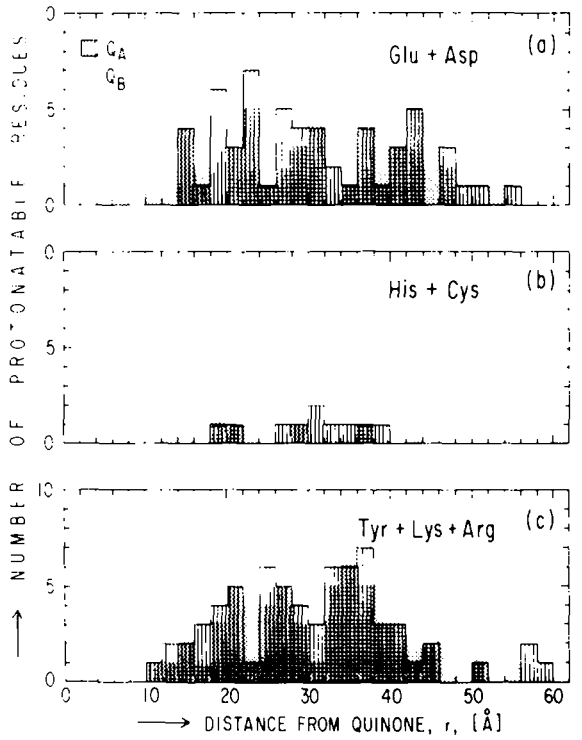

Fig. 13. Number of protonatable residues at distance r from Q_A (striped histograms) and Q_B (stippled histograms). Only residues whose protonatable atoms have accessible surface areas are included. Separate histograms are presented for residues that normally titrate at low pH (a), neutral pH (b), and high pH (c). Distances, obtained from the coordinates of the crystal structure [7,8], are between the center of the ring of the quinone and the protonatable atoms.

values suggests that the pK value of Tyr H40 is larger than its usual value.

Eqns. 16 and 17 predict significant interactions between Q_A^- or Q_B^- and more distant residues ($r \approx 20$–30 Å). The distributions of residues around the quinones have been obtained from the crystal structure [7,8] and are shown in Fig. 13. Separate histograms of the number of residues vs. the distance, r, from Q_A (striped histogram) and Q_B (stippled histogram) are presented for each of the following classes of residues: those that typically titrate at low pH (Fig. 13a), neutral pH (Fig. 13b), and high pH (Fig. 13c). Residues that have zero accessible surface area, i.e., those that are buried in the interior of the protein (e.g., the Fe^{2+} ligands [51]) have been excluded *. From the histograms (Fig. 13) and the interaction energy (Fig. 12) one can calculate the expected shifts in pK and the concomitant proton uptake. One sees that the protonation associated with the reduction of Q_A or Q_B can be due to the effect of many far-away residues rather than due to a few nearby ones. For example, the model predicts that the four His/Cys residues that are 18–24 Å from Q_B (Fig. 13b) each have an interaction with Q_B^- equivalent to approx. 0.2 pK. Their combined interaction of approx. 0.8 pK is twice that predicted for the nearest His/Cys that is 12–14 Å away.

Since D is approx. 25 Å from Q_A and Q_B (measured between the centers of the cofactors [7]), the model suggests that some residues interacting with Q_A^- and Q_B^- might also interact with D^+. Some of the same residues could, therefore, be involved in the proton release from D^+ and the proton uptake by Q_A^- and Q_B^-. An interaction of Q_A^-, Q_B^- and D^+ with the same residues would make the proton release from D^+ dependent on whether Q_A or Q_B is reduced. This could account for the small difference between the two sets of data in Fig. 10.

A calculation of the proton uptake of all the residues as a function of pH (assuming typical pK values) gave proton uptake values that were several times larger than the measured ones (McPherson, P.H., Okamura, M.Y. and Feher, G., unpublished data). We believe that this discrepancy is due to the neglect of interactions between charged residues and screening by counterions (K^+ and Cl^-). Note that a protonated residue will inhibit the protonation of a nearby interacting residue, thereby reducing the observed proton uptake (for a discussion of interacting vs. non-interacting residues see for example Ref. 53). The effect of ionic screening on the interaction energy between two charges in a protein approx. 15 Å apart has been investigated experimentally by Russel et al. [49]. Their results indicate that an increase in the ionic strength from 0 mM (assumed in our calculation) to 50 mM (used in our measurements) causes a decrease of approx. 35% in the interaction energy.

* The total number of residues with a protonatable side chain is 166, of which 31 were excluded from Fig. 13. Some of these buried residues could protonate if they are accessible to solution via a proton network, or 'bucket brigade', as discussed in a later section. Excluding them from Fig. 13 does not basically affect our conclusions.

Relation of the proton uptake by the semiquinone Q_B^- to the direct protonation of the doubly reduced quinone Q_B^{2-}

The free energy associated with the charge separation in the RC drives the translocation of protons across the membrane, thereby forming a chemi-osmotic potential (for reviews, see Refs. 12 and 13). The mechanism of this process has not been worked out in detail. It is believed that the doubly reduced quinone Q_B^{2-} accepts two protons from the solvent forming the quinol Q_BH_2, which dissociates from the RC. As we discussed in this work, Q_B is not protonated directly after receiving the first electron; the direct protonation is thought to take place only after the transfer of the second electron [11]. Do the residues that take up protons during the transfer of the first electron play a role in this direct proton uptake? One possibility is that some of them form a 'bucket brigade' that shuttles protons from solution during the direct uptake [54]. This hypothesis is being investigated using information obtained from the three-dimensional structure [54] and site-specific mutation of amino acid residues of the RC (Paddock, M.L., Rongey, S.H., Feher, G. and Okamura, M.Y., Work in progress). An alternate mechanism for the direct protonation of Q_B would be a solvent channel connecting Q_B to the surface of the RC. An examination of the RC structure revealed no such channel [54]. It is possible, however, that structural changes occur when Q_B is doubly reduced.

Appendix A. Derivation of the relation between proton uptake and free energy change (Eqn. 10)

We used Eqn. 10 to calculate the pH dependence of the standard free-energy change, $\Delta G^0_{Q\to Q^-}$, from the proton uptake, $\Delta H^+_{Q\to Q}$. Eqn. 10 can be obtained from the following general expression derived by Wyman [55] (Eqn. 7.4 in Ref. 55):

$$\left(\frac{\partial \Delta G}{\partial \mu_X}\right)_{n_1, n_2, \ldots} = -\Delta X \qquad \text{(A-1)}$$

where ΔG is the free-energy change and ΔX the amount (mole fraction) of uptake of an arbitrary ligand, X, for a macromolecular reaction; μ_X is the chemical potential of X. The subscripts n_1, n_2, etc. refer to the concentrations of the product and reactant species. Note that if ΔG is taken to be a standard free-energy change, i.e., $\Delta G^0_{Q\to Q^-}$, the condition of constant n_1, n_2, etc. is satisfied because the standard states of products and reactants are defined for constant concentrations of 1 molar. As pointed out by Wyman [55], Eqn. A-1 is completely general; it does not depend on the number of binding sites of X or whether they interact. In our case, the ligand is H^+ and its uptake denoted by $\Delta H^+_{Q\to Q^-}$. The chemical potential μ_{H^+} of H^+ is defined as:

$$\mu_{H^+} = \mu^0_{H^+} + kT \ln(\gamma_{H^+}[H^+]) \qquad \text{(A-2)}$$

where γ_{H^+} and $[H^+]$ are the activity coefficient and concentration of H^+, respectively, and $\mu^0_{H^+}$ is a constant. Since pH is defined by $pH = -{}^{10}\log(\gamma_H \cdot [H^+])$ (see, e.g., Ref. 36), Eqn. A-2 can be written:

$$\mu_{H^+} = \mu^0_{H^+} - (\ln 10)\cdot kT \cdot pH \qquad \text{(A-3)}$$

From Eqn. A-3, one obtains for the partial derivative in Eqn. A-1:

$$\frac{\partial}{\partial \mu_{H^+}} = \frac{\partial pH}{\partial \mu_{H^+}} \frac{\partial}{\partial pH} = -\frac{1}{(\ln 10)\cdot kT} \frac{\partial}{\partial pH} \qquad \text{(A-4)}$$

Rewriting Eqns. A-1 and A-4 in terms of $\Delta G^0_{Q\to Q}$, $\Delta H^+_{Q\to Q^-}$, and pH one obtains:

$$\frac{\partial \Delta G^0_{Q\to Q^-}}{\partial pH} = (\ln 10)\cdot kT \cdot \Delta H^+_{Q\to Q^-} \qquad \text{(A-5)}$$

Eqn. 10 is obtained by integrating Eqn. (A-5) *.

Acknowledgements

We thank E.C. Abresch for preparing the reaction centers, M. Schönfeld and D. Kleinfeld for help during the early stages of this work, D. Fredkin and A. Warshel for helpful discussions, and J.P. Allen and D.C. Rees for valuable discussions and for their help in constructing Fig. 13. This work was supported by the National Science Foundation (DMB 85-18922).

References

1 Feher, G. and Okamura, M.Y. (1978) in The Photosynthetic Bacteria (Clayton, R.K. and Sistrom, W.R., eds.), pp. 349–386, Plenum Press, New York.

* $(\ln 10)\cdot kT$ at room temperature (300 K) is 60 meV.

2 Okamura, M.Y., Feher, G. and Nelson, N. (1982) in Photosynthesis: Energy Conversion by Plants and Bacteria, Vol. I (Govindjee, ed.), pp. 195–272, Academic Press, New York.
3 Parson, W.W. (1987) in Photosynthesis (Amesz, J., ed.), pp. 43–61, Elsevier Science Publishers, Amsterdam.
4 Williams, J.C., Steiner, L.A., Ogden, R.C., Simon, M.I. and Feher, G. (1983) Proc. Natl. Acad. Sci. USA 80, 6505–6509.
5 Williams, J.C., Steiner, L.A., Feher, G. and Simon, M.I. (1984) Proc. Natl. Acad. Sci. USA 81(23), 7303–7307.
6 Williams, J.C., Steiner, L.A. and Feher, G. (1987) Proteins 1, 312–325.
7 Allen, J.P., Feher, G., Yeates, T.O., Komiya, H. and Rees, D.C. (1987) Proc. Natl. Acad. Sci. USA 84, 5730–5734.
8 Allen, J.P., Feher, G., Yeates, T.O., Komiya, H. and Rees, D.C. (1987) Proc. Natl. Acad. Sci. USA 84, 6162–6166.
9 Parson, W.W. and Ke, B. (1982) in Photosynthesis: Energy Conversion by Plants and Bacteria, Vol. I (Govindjee, ed.), pp. 331–385, Academic Press, New York.
10 Kirmaier, C. and Holten, D. (1987) Photosynth. Res. 13, 225–260.
11 Wraight, C.A. (1982) in Function of Quinones in Energy-Conserving systems (Trumpower, B.L., ed.), pp. 181–197, Academic Press, New York.
12 Ort, D.R. and Melandri, B.A. (1982) in Photosynthesis: Energy Conversion by Plants and Bacteria, Vol. I (Govindjee, ed.), pp. 537–587, Academic Press, New York.
13 Cramer, W.A. and Crofts, A.R. (1982) in Photosynthesis: Energy Conversion by Plants and Bacteria, Vol. I (Govindjee, ed.), pp. 387–467, Academic Press, New York.
14 Wraight, C.A. (1979) Biochim. Biophys. Acta 548, 309–327.
15 Kleinfeld, D., Okamura, M.Y. and Feher, G. (1984) Biochim. Biophys. Acta 766, 126–140.
16 Cogdell, R.J., Prince, R.C. and Crofts, A.R. (1973) FEBS Lett. 35, 204–208.
17 Wraight, C.A., Cogdell, R.J. and Clayton, R.K. (1975) Biochim. Biophys. Acta 396, 242–249.
18 Maróti, P. and Wraight, C. (1985) Biophys. J. (Abstr.) 47, 5a.
19 Maróti, P. and Wraight, C.A. (1986) Proceedings of the VIIth International Congress of Photosynthesis, Poster Abstr. No. 205–311.
20 Maróti, P. and Wraight, C.A. (1987) in Progress in Photosynthesis Research (Biggins, J., ed.), Vol. II, pp. 401–404, Martinus Nijhoff, Dordrecht.
21 Dutton, P.L., Leigh, J.S. and Wraight, C.A. (1973) FEBS Lett. 36, 169–173.
22 Jackson, J.B., Cogdell, R.J. and Crofts, A.R. (1973) Biochim. Biophys. Acta 292, 218–225.
23 Prince, R.C. and Dutton, P.L. (1976) Arch. Biochem. Biophys. 172, 329–334.
24 Wraight, C.A. (1981) Isr. J. Chem. 21, 348–354.
25 Rutherford, A.W. and Evans, M.C.W. (1980) FEBS Lett. 110, 257–261.
26 Clayton, R.K. and Straley, S.C. (1972) Biophys. J. 12, 1221–1234.
27 Slooten, L. (1972) Biochim. Biophys. Acta 275, 208–218.
28 Verméglio, A. and Clayton, R.K. (1977) Biochim. Biophys. Acta 461, 159–165.
29 Feher, G., Okamura, M.Y. and McElroy, J.D. (1972) Biochim. Biophys. Acta 267, 222–226.
30 McPherson, P.H., Okamura, M.Y., Feher, G. and Schönfeld, M. (1987) Biophys. J. (Abstr.) 51, 125a.
31 Margoliash, E. and Frohwirt, N. (1959) Biochem. J. 71, 570–572.
32 Straley, S.C., Parson, W.W., Mauzerall, D.C. and Clayton, R.C. (1973) Biochim. Biophys. Acta 305, 597–609.
33 Okamura, M.Y., Debus, R.J., Kleinfeld, D. and Feher, G. (1982) in Function of Quinones in Energy-Conserving Systems (Trumpower, B.L., ed.), pp. 299–317, Academic Press, New York.
34 Okamura, M.Y., Isaacson, R.A. and Feher, G. (1975) Proc. Natl. Acad. Sci. USA 72, 3491–3495.
35 McElroy, J.D., Mauzerall, D.C. and Feher, G. (1974) Biochim. Biophys. Acta 333, 261–288.
36 Bates, R.G. (1973) Determination of pH; theory and practice, 2nd Edn., John Wiley, New York.
37 Czerlinski, G.H. and Dar, K. (1971) Biochim. Biophys. Acta 234, 57–61.
38 Swallow, A.J. (1982) in Function of Quinones in Energy Conserving Systems (Trumpower, B.L., ed.), pp. 59–72, Academic Press, New York.
39 Ho, C. and Russu, I.M. (1987) Biochemistry 26, 6299–6305.
40 McPherson, P.H., Arno, T., Okamura, M.Y. and Feher, G. (1988) Biophys. J. (Abstr.) 53, 271a.
41 Feher, G., Arno, T.R. and Okamura, M.Y. (1988) in The Photosynthetic Bacterial Reaction Center: Structure and Dynamics, Vol. 149, (Breton, J., ed.), pp. 271–287, Plenum Press, New York.
42 Arata, H. and Parson, W.W. (1981) Biochim. Biophys. Acta 638, 201–209.
43 Woodbury, N.W., Parson, W.W., Gunner, M.R., Prince, R.C. and Dutton, P.L. (1986) Biochim. Biophys. Acta 851, 6–22.
44 Okamura, K., Takamiya, K. and Nishimura, M. (1985) Arch. Microbiol. 142, 12–17.
45 Takamiya, K., Iba, K. and Okamura, K. (1987) Biochim. Biophys. Acta 890, 127–133.
46 Dutton, P.L. and Prince, R.C. (1978) in The Photosynthetic Bacteria (Clayton, R.K. and Sistrom, W.R., eds.), pp. 525–570, Plenum Press, New York.
47 Cantor, C.R. and Schimmel, P.R. (1980) Biophysical Chemistry, Part 1, W.H. Freeman and Company, San Francisco.
48 Rees, D.C. (1980) J. Mol. Biol. 141, 323–326
49 Russel, A.J., Thomas, P.G. and Fersht, A.R. (1987) J. Mol. Biol. 193, 803–813.
50 Warshel, A., Russell, S.T. and Churg, A.K. (1984) Proc. Natl. Acad. Sci. USA 81, 4785–4789.
51 Yeates, T.O., Komiya, H., Rees, D.C., Allen, J.P. and Feher, G. (1987) Proc. Natl. Acad. Sci. USA 84, 6438–6442.
52 Russell, S.T. and Warshel, A. (1985) J. Mol. Biol. 185, 389–404.
53 Klotz, I.M. and Hunston, D.L. (1979) Arch. Biochem. Biophys. 193, 314–328.
54 Allen, J.P., Feher, G., Yeates, T.O., Komiya, H. and Rees, D.C. (1988) in The structure of the Photosynthetic Bacterial Reaction Center: Structure and Dynamics, Vol. 149, (Breton, J., ed.), pp. 271–287, Plenum Press, New York.
55 Wyman, J. (1964) Adv. Protein Chem. 19, 223–286.